Gehring, Kai; Schaudt, Paul

Working Paper

Insuring Peace: Index-Based Livestock Insurance, Droughts, and Conflict

CESifo Working Paper, No. 10423

Provided in Cooperation with:
Ifo Institute – Leibniz Institute for Economic Research at the University of Munich

Suggested Citation: Gehring, Kai; Schaudt, Paul (2023) : Insuring Peace: Index-Based Livestock Insurance, Droughts, and Conflict, CESifo Working Paper, No. 10423, Center for Economic Studies and ifo Institute (CESifo), Munich

This Version is available at:
https://hdl.handle.net/10419/279172

CESifo WORKING PAPERS

10423
2023

May 2023

Insuring Peace: Index-Based Livestock Insurance, Droughts, and Conflict

Kai Gehring, Paul Schaudt

CESifo

Impressum:

CESifo Working Papers
ISSN 2364-1428 (electronic version)
Publisher and distributor: Munich Society for the Promotion of Economic Research - CESifo GmbH
The international platform of Ludwigs-Maximilians University's Center for Economic Studies and the ifo Institute
Poschingerstr. 5, 81679 Munich, Germany
Telephone +49 (0)89 2180-2740, Telefax +49 (0)89 2180-17845, email office@cesifo.de
Editor: Clemens Fuest
https://www.cesifo.org/en/wp
An electronic version of the paper may be downloaded
· from the SSRN website: www.SSRN.com
· from the RePEc website: www.RePEc.org
· from the CESifo website: https://www.cesifo.org/en/wp

CESifo *Working Paper No. 10423*

Insuring Peace: Index-Based Livestock Insurance, Droughts, and Conflict

Abstract

We provide novel evidence of how an innovative market-based solution using remote-sensing technology can mitigate conflict. Droughts are a major driver of conflict in Africa, particularly between nomadic pastoralists and sedentary farmers, and climate change is predicted to intensify this problem. The Index-Based Livestock Insurance (IBLI) scheme piloted in Kenya provides automated, preemptive payouts to pastoralists affected by droughts. Combining plausibly exogenous variation in rainfall and the staggered roll-out of IBLI in Kenya over the 2001-2020 period, we find that IBLI strongly reduces drought-induced conflict. One key mechanism is that insured pastoralists travel less far away from their ancestral homelands, reducing conflicts over scarce resources in contested areas. This suggests that market-based solutions are a promising pathway to mitigate conflict beyond difficult institutional reforms and raises the question of how governments can support the adoption of such schemes for underprivileged groups through subsidies or other campaigns.

JEL-Codes: D740, G220, G520, O130, Q340, Q540.

Keywords: conflict, conflict resolution, climate change, droughts, pastoralism, insurance, ICT, resources.

Kai Gehring
Department of Economics &
Wyss Academy for Nature
University of Bern / Switzerland
kai.gehring@unibe.ch

Paul Schaudt
Department of Economics
University of St. Gallen / Switzerland
paul.schaudt@unisg.ch

This version: May 9, 2023
We thank Nathaniel Jensen for kindly sharing his data on insurance rollout and payments with us. Dylan Philippe and Amelia Libeau provided excellent research assistance. Paul Schaudt acknowledges funding from the Swiss National Science Foundation Ambizione project PZ00P1208916. We are grateful for helpful suggestions by Dominic Rohner and Roland Hodler, as well as comments from seminar participants at the University of St.Gallen, and the EPCS 2023 conference.

1. Introduction

Mitigating drought-induced conflict pressure in fragile regions of the world is a crucial public policy challenge for the next decades. Recent research highlights that tensions between nomadic pastoralists and sedentary farmers are a root cause of a high share of all violent conflict, particularly in Africa (Eberle et al., 2020; McGuirk and Nunn, 2023). This type of conflict erupts because droughts intensify competition for scarce resources and force pastoralists to migrate further away from their traditional grazing grounds in areas inhabited by farmers. Such conflicts are amplified by agricultural intensification (more fencing, denser fields, less open areas (see McGuirk and Nunn, 2022), and by a higher frequency and severity of droughts linked to climate change (IPCC, 2022). Eberle et al. (2020) estimate that climate-induced conflict in Africa will increase by up to a third without countervailing measures.

This paper provides the first, to the best of our knowledge, quasi-experimental evidence that index-based livestock insurance (IBLI) can substantially mitigate drought-induced farmer-herder conflicts. Market-based mechanisms are crucial complements to reforms of political institutions, which are highly persistent and unlikely to adapt at the speed necessary to cope with climate change. IBLI leverages advances in remote sensing techniques to develop local forage proxies, which allow offering index-based insurance to previously uninsurable pastoralists. IBLI avoids costly controls by automatically triggering payouts once pre-determined remotely sensed drought measures are crossed. Moreover, this enables preemptive payouts before livestock loss occurs (Vrieling et al., 2014) and avoids manipulations of the payout amount. IBLI was piloted in Northern Kenya, then rolled out through the semi-arid and arid areas of Kenya, and is now expanding across East Africa (Fava et al., 2021).

Our main specification examines the reduced-form effect of IBLI coverage on drought-induced violent conflict in Kenya over the 2001-2020 period. Our dependent variable uses the Armed Conflict Location and Event Dataset (ACLED Raleigh et al., 2020) to measure the probability of conflict in 0.1 $\times$ 0.1-degree grid-cells (roughly 10 x 10 km at the equator). The treatment variable combines the staggered roll-out of IBLI with exogenous changes in drought intensity in the neighborhood of a cell. To reflect the declining likelihood of pastoralist migration from potentially drought-affected neighborhood cells, their weight decreases in distance. Our main results suggest that the drought-conflict semi-elasticity is reduced by between 14% and 26% in regions with higher insurance coverage. Quantifying the conflict-mitigation externality of IBLI is politically important because it is relevant to evaluate the optimal level of government subsidies of the program.

There are two main concerns when evaluating such an insurance scheme. The first endogenous payouts manipulated or delayed due to conflict are not a concern because pre-defined satellite-based drought proxies trigger IBLI payouts. The second concern is that the insurance's initial choice and roll-out pattern were linked not just to the likelihood of conflict but also to the degree to which droughts are likely to trigger conflict in an area. The mere conflict likelihood – and other time-invariant factors – would be captured by our battery of fixed effects, but the second concern could introduce a bias. All available information suggests that improving pastoralist well-being and solving technical challenges were the key factors influencing the initial IBLI location choice and the roll-out (Fava et al., 2021). We show

empirically that neither IBLI eligibility, ever receiving coverage, or the timing of receiving coverage during our sample period depends on the prior drought-conflict sensitivity of an area. A placebo test further reveals that our treatment variable does not affect the drought-conflict relationship during the 2001-2009 period, before the initial IBLI pilot.

Our results are robust to varying core assumptions and data. First, while our main specification uses rainfall deficit as the proxy for drought, we also employ a more comprehensive Aridity Index that takes temperature variation into account, as well as a proxy for phytomass availability (the Dry Matter Productivity–DMP) as alternative proxies for droughts. Second, we show that our results also hold using various distance decays. Third, our results are robust to using alternative conflict measures. Fourth, we interact the drought measures with time-invariant characteristics of the cell or the neighborhood cells as additional controls.

We then turn to the mechanisms. Let us start with an example to illustrate through which channels droughts lead to conflict. Orma and Wardey pastoralists and the Pokomo farmers are three groups that all rely in some way on the Tana River Delta, an important Kenyan wetland.[1] Water and grazing grounds are scarce resources that the groups require access to. Land rights are complex and contested, including rights of passage, and migratory movements by the pastoral groups do occasionally lead to the destruction of Pokomo crops. Hence, occasional conflicts among the two pastoralist groups or between pastoralists and the Pokomo sporadically occurred since the 17th century. During years with sufficient rain, however, traditional conflict resolution mechanisms such as community-led negotiations and resource-sharing agreements often avoid or stop conflict from escalating.

Droughts affect this fragile equilibrium and the likelihood of conflict in several ways. First, both farmers and pastoralists are materially worse off in a drought. Following the opportunity-cost of fighting hypothesis, reduced material wealth, all else equal, increases the likelihood of conflict. Second, droughts further reduce the available resources to all groups, leading to a rapacity effect with groups more aggressively competing for those resources. Finally, in drought years, the pastoral groups - desperately trying to keep their cattle alive - migrate into Pokomo areas more deeply and frequently (Andres, 2013), potentially interrupting growing seasons (McGuirk and Nunn, 2023). In summary, droughts affect conflict through lower opportunity costs, a stronger rapacity effect, and more frequent and longer migration movements that increase the possibility of unexpected contact between groups.

We can shed some light on the extent to which IBLI seems to mitigate conflict through these mechanisms. We provide evidence that less migratory pressure plays a key role. In line with (Eberle et al., 2020) we match conflict actors to ethnic homelands (Murdock, 1967) and show that IBLI reduces the distance between the centroid of a group's homeland and conflict events involving that group. Moreover, Jensen et al. (2017) finds that IBLI helps to smooth and increase pastoralists' incomes, fostering investments in livestock health services and increasing milk productivity. This increases the opportunity costs of fighting. The higher productivity per cow can lead to a quantity-quality trade-off and, in equilibrium, smaller herd sizes that

[1] See https://www.hrw.org/news/2012/09/13/kenya-investigate-all-politicians-tana-river-violence for details.

mitigates the rapacity effect.

Many African countries face challenges similar to the problems of pastoralists and sedentary farmers in Kenya's semi-arid and arid landscapes. Pastoralism is practiced in 43% of the African landmass, covering 36 countries, and is the livelihood of about 268 million people (FAO, 2018). In Kenya, large areas of land are (traditionally) dedicated to pastoralism, particularly in the northern and eastern regions. Pastoralists depend on the natural environment for their livelihoods, primarily raising cattle, sheep, and goats. One can already observe now that more frequent droughts reduced water availability and forage quality for their livestock. Climate change is predicted to further amplify those challenges, particularly in the Sahel and Horn of Africa. Hence, the findings of this study are relevant for understanding the potential of IBLI as an ICT tool and conflict-mitigating intervention in many other settings with similar conditions and features.

Our results relate to several strings of related literature. First, understanding the potential of index-based insurance for drought-induced conflict contributes to recent quasi-experimental and experimental evidence on the potential of conflict-mitigating interventions (see overviews in Blattman, 2022; Rohner, 2022). Prior studies exploring mitigating drought-induced conflict have focused on political solutions such as power sharing and formal land dispute resolution mechanisms (McGuirk and Nunn, 2023; Eberle et al., 2020, , referred to as MN and ERT for the remainder of the study). In particular, in settings where distrust among groups makes political agreements and reforms hard to reach, market-based solutions might be easier to implement. Key challenges in insuring traditional groups in remote locations are take-up and affordability. By showing that the insurance has a positive externality in terms of less conflict that benefits more groups than just the pastoralists themselves, we provide an argument to foster uptake with further subsidies.

Second, our results highlight that targeted – and potentially subsidized – index-based insurance has the potential to weaken the link between weather shocks and conflict, even in fragile conflict-prone settings. This contributes to a large literature linking economic shocks, resources, and conflict (e.g., Morelli and Rohner, 2015; Dube and Vargas, 2013; Berman and Couttenier, 2015; Bazzi and Blattman, 2014; Berman et al., 2017; McGuirk and Burke, 2020; Gehring et al., 2023; Hodler et al., 2023). Land is a key resource, especially if there are competing claims for land use. Weather shocks, potentially amplified by climate change, often create or intensify conflict in such settings (Miguel et al., 2004; Couttenier and Soubeyran, 2014; Koubi, 2019). Moreover, farmer-herder conflicts in Africa usually pit members of different ethnic groups against one another, adding an ethnic dimension to the violence that creates its own conflict dynamics (Michalopoulos and Papaioannou, 2016; Moscona et al., 2020; Cao et al., 2021).

Finally, by demonstrating the potential of remote-sensing-based insurances with automated payouts, we contribute to a growing literature studying technology for development (ICT) (Blumenstock, 2016; Fabregas et al., 2019). ICT ranges from simple tools like SMS messaging that help farmers increase yields (Casaburi et al., 2019) to hotline services that solve free-riding problems (Casaburi et al., 2019), and the use of remote-sensing technology for insurance design (Benami et al., 2021). Our results most directly relate to and

complement Jensen et al. (2017), who show the direct positive effect of IBLI on pastoralist groups. One big challenge is insufficient demand for insurance, which could be partly explained by high upfront costs in settings with liquidity constraints and present bias (see Casaburi and Willis, 2018). Incomplete land markets pose another challenge, but (Acampora et al., 2022) show that subsidies can help to cope with these frictions. Our results further justify well-designed subsidies and other measures to foster insurance adaption.

The remainder of the paper is structured as follows. Section 2 introduces our setting, study setup, and main variables. Section 3 discusses our identification strategy. Section 4 presents our results. Section 5 concludes and discusses implications for public policy.

2. Setting and data

2.1. Setting and data sources

Our units of analysis are grid cells of 0.1 $\times$ 0.1 degree (roughly 10 x 10 km at the equator) covering the entire landmass of Kenya.[2] The temporal dimension comprises 12-month periods starting in October and ending in September of the following year, covering March 2001 until February 2020. In Kenya, the short rains and dry season (SRSD), lasts from October to February, and the long rains and dry season (LRLD), from March to September. Defining periods this way ensures that each period reflects both seasons, which is important to mimic the timing of insurance availability and payouts within our temporal units.[3] Moreover, it makes sure that we capture a full migratory cycle of pastoralists (see panel A of Figure I for a sketch of some routes). The combination of cells and periods results in 94300 cell periods, which are our units of observation. Summary stats and sources for all variables are provided in Online Appendix A.

Conflicts constitute a key challenge for development in Kenya, and the frequency of recorded conflict events has increased over the last two decades. The three most relevant types of conflicts are political violence between different ethnic groups, terrorism related to the Somalia-based Al-Shabab militia, and conflicts involving farmers and pastoralists (often having an ethnic component). Depending on the definition, Kenya is home to over 40 ethnic groups, and ethnic tensions are often linked to conflict.

To ensure comparability to the most closely related literature, our main conflict data source is the Armed Conflict Location and Event Data (ACLED, Raleigh et al., 2020), as in ERT and MN and the wider literature (e.g., Berman and Couttenier, 2015; Berman et al., 2017). ACLED is the most comprehensive source of conflict event data in Africa and does not bottom censor events compared to other sources. Thus, ACLED is ideal for capturing both high- and low-intensity clashes between pastoralists (and farmers) during droughts.[4] ACLED contains

[2] We chose the native resolution of our precipitation data as a grid, which is much more granular compared to other studies which rely on grid-cells of 0.5 or 0.25-degree grid-cells (e.g., Eberle et al., 2020; Berman et al., 2021). The more granular grid allows us to be flexible with our drought exposure definition.

[3] When we refer to the year 2001, we mean the period from March 2001 until February 2002.

[4] Comparable sources such as UCDP/PRIO (Sundberg and Melander, 2013) operate with fatality (battle-related death threshold) events need to pass to be included in the database, resulting in only one-seventh of event coverage

information on the date and type of conflict events, the involved actors (e.g., government, tribal groups, civilians), and the geolocation. We follow MN and use the information on all conflict events as our baseline measure, but also construct sub-indicators focusing on specific conflict types and actors as in Mn and ERT.

Index-based livestock insurance (IBLI) was piloted in Marsabit county in Kenya. Leveraging remotely sensed information on pasture availability using the Normalized Difference in Vegetation Index (NDVI), IBLI automatically triggers payouts, proportional to the estimated loss function, to insured pastoralists when a threshold is crossed within an insurance area (see Fava et al., 2021, for a detailed program description). Improvements in forage predictions allow for early payouts (Vrieling et al., 2014; Fava and Vrieling, 2021) that are preemptive, designed to avoid loss of assets like cattle rather than compensating for damages (Chantarat et al., 2013). The automated triggering of payouts to all insured households within an insurance area ensures cost-effective monitoring and transparent distribution. The International Livestock Research Institute (ILRI) independently calculates the index and communicates insurance triggering, while private Kenyan insurance agencies offer insurance plans and disburse payouts primarily through mobile banking (MPesa).[5]

In 2015, the Kenyan Government began to subsidize IBLI, and labeled it domestically the Kenyan Livestock Insurance Program (KLIP) (Fava et al., 2021). As part of a private-public arrangement, the government fully subsidizes coverage for up to five tropical livestock units (TLUs), with a TLU corresponding to one cattle or 10 goats/sheeps. Panel B of Figure I provides information on the spatial-temporal roll-out of IBLI availability across the 145 insurance districts, with an average size of $2817km^2$ (about 9/10 the size of a PRIO grid-cell).[6] As of 2019, IBLI cover around 18000 households in eight arid and semi-arid counties that host substantial pastoral populations (roughly 60% of the pastoral counties).[7] A further expansion into the other pastoral counties is planned but not concluded as of 2022.[8]

Droughts occur regularly in Kenya (although they become more frequent) and are usually concentrated in arid and semi-arid regions, predominantly hosting the country's pastoral populations. Our main proxy for drought intensity is the reduction in rainfall (rainfall deficit) across grid-cells in millimeters over a year. The data comes from NASA's GMP product (Huffman et al., 2017). It provides monthly rainfall sums at a spatial resolution of 0.1 degrees. In robustness test we also use a phytomass proxy built on Dry Matter Productivity (DMP) (Copernicus Global Land Service, 2019), which is more directly related to the availability of

for Kenya.

[5]Those companies include UAP Insurance Company, Oromia Insurance Company (OIC), APA Insurance Ltd., and Takaful Insurance of Africa (see https://ibli.ilri.org/index/.)

[6]Borders highlighted with the black dashed lines in Figure I. The areas are designed based on local knowledge of pastoralists' migration and camp settlement patterns (see Chelanga, Khalai, Fava, and Mude, Chelanga et al.).

[7]We define pastoral areas based on their counties membership in the "Pastoral Parliamentary Group" (PPG) (highlighted as green borders in panel B of Figure I, see https://dlci-hoa.org/ppg/overview(09/26/2022). Panels A and B of Figure A-1 in Online Appendix A show that pastoral classified counties correlate positively with the rangeland share of a county and negatively with the agricultural share.

[8]Data for the time-varying insurance availability has been kindly shared with us by the International Livestock Research Institute (ILRI).

forage, and an aridity index (Abatzoglou et al., 2018), which also reflects temperature, soil, and wind conditions.[9]

We chose a rainfall-based measure over more complex measures attempting to proxy directly for available forage-based because it is (i.) readily available with high spatial and temporal resolution, (ii.) widely employed in the literature and easily interpreted, and (iii.) not influenced by local human behavior that might also be related to conflict, e.g., continuous overgrazing that depresses forage availability over time.

2.2. Variable construction

As evident in the example of the Orma pastoralists, we need to create variables at different levels to capture the situation's complexity in the best possible way. We first create variables at the level of the cell itself, e.g., to capture conflict in that cell as our main outcome. MN show that droughts in surrounding areas are the most important driver of farmer-herder conflict. Hence, we must also create neighborhood-level variables that capture the detrimental effect of droughts and the potentially conflict-mitigating effect of IBLI coverage on conflict in the cell itself.

The logic of our approach is simple: The further away a neighborhood cell j is from cell i, the less likely it is that a drought in cell j will affect conflict in cell i, on average. Panel A of Figure I highlights three important insights. First, maximum travel distances differ substantially between regions and pastoralist groups, ranging from around 50km to over 250km. Second, migration routes are not fixed, but rather rough corridors that alter in response to region- and year specific circumstances (see Flintan et al., 2013). Third, traveling further away from traditional pastoralist land is costly and risky, so pastoralists undertake such journeys only when necessary.

We define a tractable probabilistic measure that captures the decreasing influence of droughts in neighborhood cells j further away from cell i. Specifically, we use inverse-distance weighting to compute the weighted average of our treatment variables x of all surrounding cells $!i$ for a cell i as follows

$$x \text{ neighborhood}_i = \frac{\sum_{j \neq i} x_j \cdot d_{i,j}^{-1}}{\sum_{j \neq i} d_{i,j}^{-1}}, \tag{1}$$

where x_j is the value of the variable in cell j, $d_{i,j}$ is the distance between cells i and j, and x neighborhood$_i$ is the inverse distance weighted average of the variable for cell i. In contrast to alternatives like fixed buffer zones or uniform cut-offs for defining a neighborhood, inverse distance weighting allows us to accommodate the considerable heterogeneity in pastoralist migration routes across Kenya. For our main measures, we employ a decay of $d_{i,j}^{-1}$, but also use a variety of lower and higher inverse distance weights for robustness tests.

[9] Both measures are rather strongly correlated with the rainfall deficit, as can be seen in Table A-2).

FIGURE I
Conflict, insurance (IBLI) coverage in space

(A) Migration routes sketch

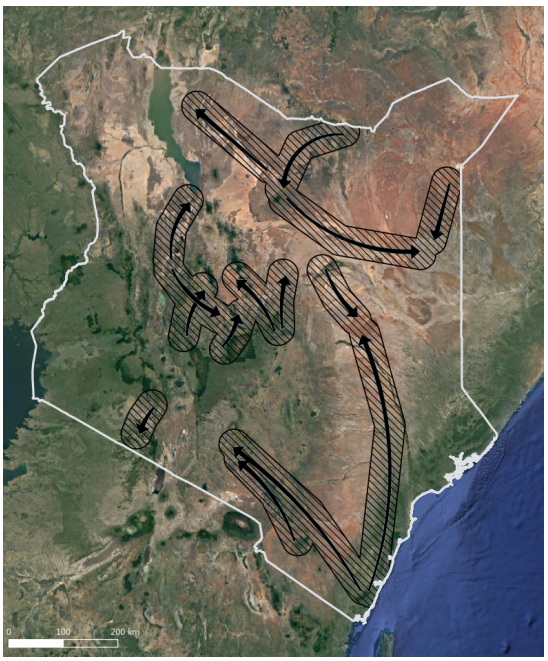

(B) Conflict and insurance across space

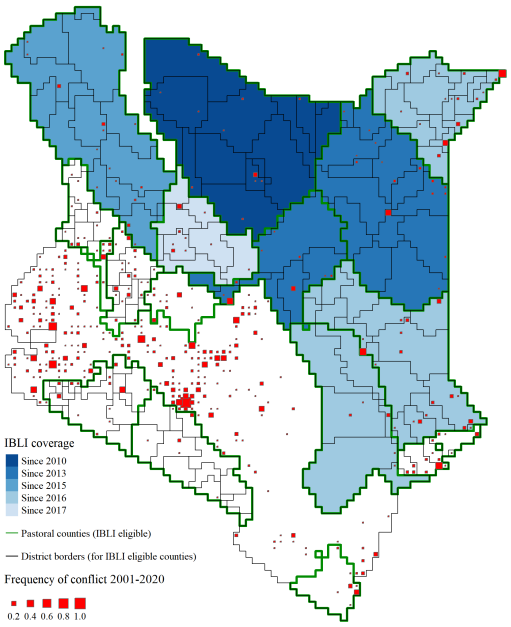

(C) IBLI coverage (2019)

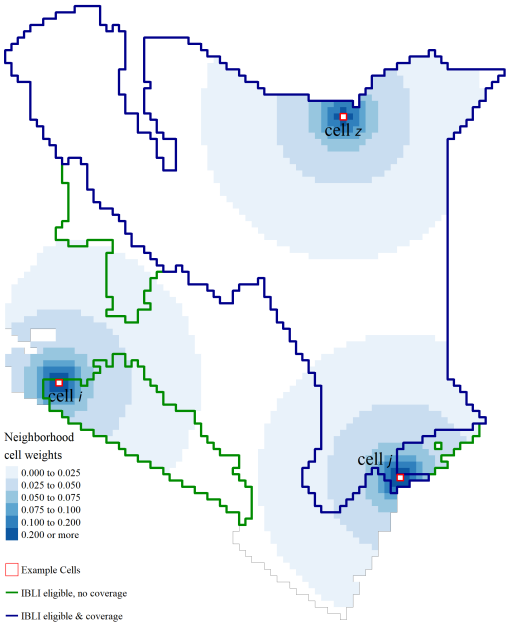

(D) IBLI coverage neighborhood (2019)

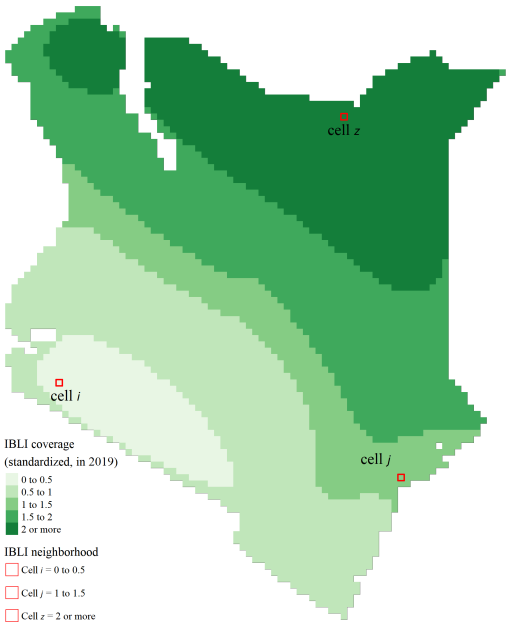

Notes: Panel A sketches some of the migration routes during the long rain and dry season of 2013 within Kenya as depicted in figure 2 of Flintan et al. (2013). Panel B plots the frequency of conflict events across cells (red squares) and the roll-out of IBLI coverage across locations in Kenya. Black lines highlight insurance district borders. Green lines indicate counties with sizable pastoral populations (defined as a member county of the Pastoralist Parliamentary Group (PPG)). Panel C plots the IBLI coverage in 2019 (blue border encompassing already covered areas and green borders not yet covered areas) and the neighborhood weights based on the 1/distance decay for three example cells (i,j, and z). Brighter shades of blue indicate smaller weights, while darker shades indicate higher weights. Panel D plots our standardized neighborhood IBLI coverage measure in 2019 across cells. The different variables are processed at a $0.1^\circ \times 0.1^\circ$ grid-cell level. Index-Based Livestock Insurance (IBLI) coverage is given by the International Livestock Research Institute (ILRI) and conflict data from ACLED (Raleigh et al., 2020).

Panel C of Figure I illustrates the neighborhood weights for three example cells (i,j, and z) and IBLI coverage in 2019. To provide one example of how the linear decay maps the weights, compare a direct neighbor cell with a cell 150km away. Cells with a distance of 150km each receive a weight of 0.025 percentage points. That means we account for the possibility that a faraway drought might cause pastoralists to move into an area, but the influence of each neighborhood cell becomes considerably smaller. However, even cells further away from example cell j will still have a positive but small impact on the neighborhood exposure of cell i.

Conflict is an indicator variable equal to one if at least one conflict event is recorded in a cell-year, and zero otherwise. The conflict data comes from the Armed Conflict Location and Event Data (ACLED Raleigh et al., 2020). We follow MN and use all conflict event types from ACLED as our baseline measure, but also construct sub-indicators focusing on conflict involving the government or specific event types and other actors (as in ERT). Conflict in our analysis is measured at the level of the cell itself. Panel B of Figure I plots the share of years in which a cell experiences at least one conflict incident between 2001 and 2020 as red dots.

IBLI is an indicator variable that equals one if the centroid of a grid-cell is located within an insurance district that already offers IBLI in a year, and zero otherwise.

IBLI neighborhood weighs IBLI coverage for cells j surrounding cell i by ($distance_{i,j}^{-1}$). We z-standardize the IBLI neighborhood measure to allow for an easier interpretation of the inverse distance weighted values. The resulting neighborhood IBLI coverage intensity across cells in 2019 is plotted in panel D of Figure I.

Rain deficit is the log of average rainfall in the cell during a year, provided by the corresponding raster cell from NASA GMP, multiplied by minus one to obtain a deficit interpretation.

Rain deficit neighborhood employs the same inverse distance weights approach described for *IBLI neighborhood*. The weighted average rainfall is logged and multiplied by minus one, similar to the cell level measure.

3. Empirical strategy

3.1. Main specification

Our empirical strategy builds on the approach used by MN to analyze the probability of conflict ($\text{Conflict}_{i,t}$) in a location/cell (i) during the period (t) using the following linear-probability model:

$$\begin{aligned}\text{Conflict}_{i,t} =& \beta_1 \text{Rain deficit}_{i,t} + \beta_2 \text{IBLI}_{i,t} + \beta_3 (\text{Rain deficit}_{i,t} \times \text{IBLI}_{i,t}) \\ &+ \delta_1 \text{Rain deficit neighborhood}_{i,t} + \delta_2 \text{IBLI neighborhood}_{i,t} \\ &+ \delta_3 (\text{Rain deficit neighborhood}_{i,t} \times \text{IBLI cover neighborhood}_{i,t}) \\ &+ \mathbf{X}'_{\mathbf{i,t}} \xi + \eta_i + \gamma_t + \epsilon_{i,t}\end{aligned} \tag{2}$$

where η_i are cell fixed-effects, absorbing the time-invariant climate zone (e.g., arid or semi-arid) or the historical presence of pastoralists, γ_t are period-fixed effects absorbing country-wide shocks (which we replace in some specification with IBLI-area-period fixed effects)[10], Rain deficit$_{i,t}$ is the log of rainfall multiplied by minus one. IBLI$_{i,t}$ is a proxy for livestock insurance coverage of a cell during a period. Our coefficients of interest are δ_1 to δ_3, capturing the spatial spillover (neighborhood) effects of drought, insurance availability, and the interaction thereof in the neighborhood of a grid-cell on the probability of conflict within it. $\mathbf{X_{i,t}}$ is a vector of time-variant exogenous cell controls with respect to conflict.

We thus estimate the semi-elasticity of a percentage point decrease in rainfall on the probability of conflict in a cell. Our quantity of interest is how IBLI coverage in the neighborhood affects the semi-elasticity of a percentage point decrease in rainfall on the probability of conflict. Ex-ante, we expect higher coverage to translate to a smaller semi-elasticity, i.e., insurance reducing the conflict effect of droughts.

3.2. Identifying variation and assumptions

In this subsection, we illustrate the quantities compared in our analysis and discuss the assumptions required for a causal interpretation. Panel A of Figure II plots the share of conflict events across cells with below and above median 2019 IBLI coverage in their neighborhood for the comparable drought years 2009 and 2019. The figure clearly shows that the relative share of events that occurs in areas with an above-median IBLI coverage in 2019 has significantly fallen (by about 50%) by the time roll-out is maximized in our sample, compared to the last year before the start of the rollout, i.e., in absence of insurance.

To causally interpret the differences and our coefficients of interest, we require some assumptions. A first key assumption is that rainfall changes should be orthogonal to IBLI coverage, i.e., rainfall trends should be similar between cells receiving IBLI coverage and those that do not. Second, there should be no secular trend that explains the mitigating effect of IBLI on the drought conflict semi-elasticity. Third, the IBLI roll-out and the following coverage in the neighborhood of cells should not be selective on the drought-conflict elasticity because both scenarios could potentially bias our effects.[11]

Panel B of Figure II shows that the rainfall trends seem to be parallel between those cells that never receive IBLI coverage, those that are not eligible for IBLI coverage, and those that

[10] IBLI-area fixed effects allow us to account for the differential impact of rainfall deficits on forage shortages on arid- and semi-arid areas compared to others, as well as for differential rainfall impacts within years, e.g., the drought in north-eastern Kenya and floods in the west of the country in 2022. Moreover, they account for static differences that determine the eligibility of a location for coverage.

[11] For example, if IBLI is targeted to save locations (i.e., locations that exhibit a low drought conflict semi-elasticity) would underestimate the effect.

FIGURE II
Placebo results & IBLI selection on conflict-rainfall semi-elasticity

(A) Conflict shares (by IBLI availability)

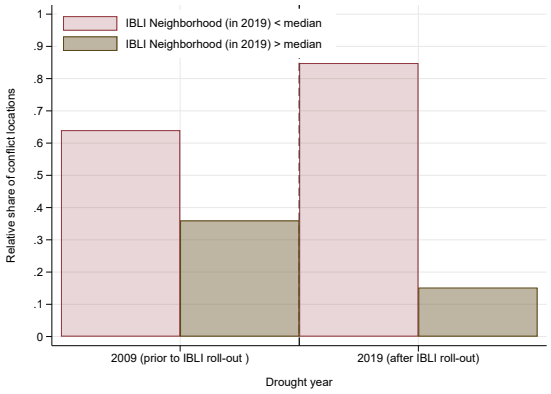

(B) Rainfall (by IBLI availability)

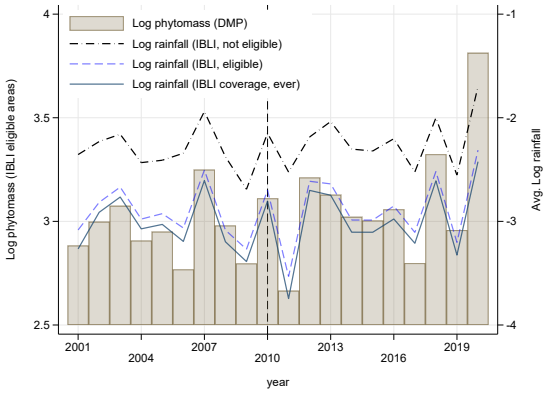

(C) Placebo

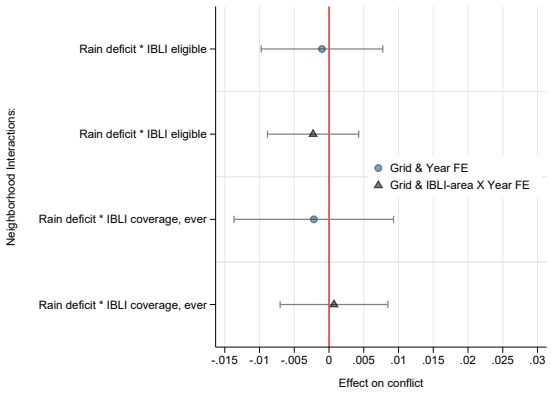

(D) IBLI selection on conflict-rain elasticity

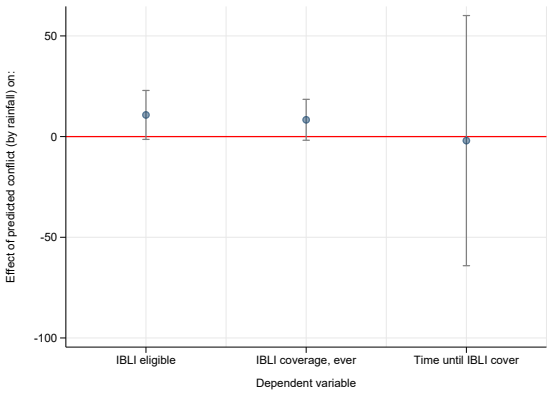

Notes: Panel A plots the share of conflict occurring in areas with above and below median IBLI coverage (in 2019) in their neighborhood for the drought years 2009 and 2019. Panel B plots the avg. rainfall for areas that are never eligible for IBLI (black dashed line), eligible areas (bright blue dashed line), and areas that receive IBLI coverage (dark blue line) over our sample period. In addition, we plot the log level of available pythomass (Dry Matter Producitivy) in pastoral areas as a proxy for forage scarcity in pastoral areas. Panel C reports the results from a placebo regression covering the period 2001 to 2009 (based on eq. 2) in we which we use IBLI eligibility (or ever IBLI coverage) instead of the time-varying coverage measure. We report the interaction coefficient of the neighborhood rainfall deficit with either insurance proxy and their 95% confidence intervals. Panel D plots the coefficient and 95% confidence intervals from regressing the IBLI eligibility dummy, the ever IBLI coverage dummy, and a time until IBLI coverage count (for those cells that receive IBLI) on the average conflict probability predicted by rainfall on the cell and its neighborhood (2001-2009). The 95% CI in panels C and D are based on Conley standard errors are implemented using the acreg package in Stata (Colella et al., 2019), with a distance cutoff of 200km. The different variables are processed at a $0.1^\circ \times 0.1^\circ$ grid-cell level. Data on rainfall comes from NASA's GMP product (Huffman et al., 2017). Index-Based Livestock Insurance (IBLI) coverage is given by the International Livestock Research Institute (ILRI) and conflict events from ACLED (Raleigh et al., 2020).

are eligible but do not receive it in our sample, and cells that obtain IBLI coverage sometime between 2010 and 2020. Despite the parallel trends, there are substantial level differences in the rainfall, which can be attributed to the location of pastoralists in semi-arid and arid areas in Kenya. The level differences are, however, not an issue for our empirical specification because our set of fixed effects leverages exclusively variation in cells over time, of which there is plenty (see panel B). In addition, panel B plots the log level of available pythomass in pastoral areas (semi-arid and arid cells). We are reassured that the rainfall correlates positively with

the amount of forage in pastoral areas, providing descriptive evidence favoring the forage shortage channel that induces migration deviations during droughts (see MN).

To test for potential underlying secular trends or potential anticipation effects of IBLI coverage, we use our main specification and run placebos tests. Specifically, we replace the time-variant *IBLI* variable with the IBLI eligible (or *ever IBLI*) equivalent and limit the estimation sample to the 2001 to 2009 period, i.e., before IBLI was available anywhere in Kenya. Panel C of Figure II plots the neighborhood interaction coefficients of those IBLI coverage proxies and the rainfall deficit (triangles representing specifications in which we add pastoral-area × year FE), and we obtain statistically insignificant point estimates that are also close to zero in terms of magnitude. Hence, locations that are more likely to receive IBLI coverage are not systematically selected based on their prior drought-conflict semi-elasticity. As an additional test for problematic selection into the treatment, we provide evidence that insurance payouts in a IBLI area are not predicted by current, past, or future conflict (see Table B-1).

Finally, we find no evidence in favor of IBLI selection with respect to the drought-conflict semi-elasticity. We test for the possibility by first regressing conflict on the rainfall deficit (in the cell and neighborhood) and the usual fixed effects, from which we obtain the predicted conflict. Panel D of Figure II clearly shows that the rainfall-predicted conflict does not predict IBLI coverage in cells. Instead, naturally, IBLI is specifically targeted toward pastoral communities, which inhabit different areas. Figure B-1 in the appendix highlights that IBLI coverage and the time until IBLI is offered are correlated with various factors that lead groups to adopt mobile herding practices in the first place.[12] We will show in robustness tests that those factors do not bias our estimates.

4. Results

4.1. Main results

Table I displays our main results, adding the respective rain deficit and IBLI variables at the cell and neighborhood level sequentially. We refrain from interpreting the cell-level variables causally and focus on the neighborhood measures. Column 1 shows that a higher rain deficit in the neighborhood, as indicated by our descriptive statistics, is indeed linked to significantly more conflict in the cell itself. Column 2 shows that, on average, more IBLI coverage in the neighborhood is associated with less conflict. Column 3 adds our main treatment variable, rain deficit interacted with IBLI in the neighborhood. The interaction coefficient is negative and statistically significant, showing that IBLI coverage reduces the conflict-inducing effect of less rainfall. While this is our preferred specification, column 4 shows that this effect holds when using IBLI-area times year fixed effects to control for the possibility that IBLI-eligible areas experience differential shocks that might be correlated with conflict and the rainfall shortage within a year.[13]

[12] There is a negative correlation with the share of farmland and a positive correlation with the share of rangeland, arid climate zones, less fertile soil, and water scarcity.

[13] The effects are stronger in fringe areas where both pastoralism and farming are practiced, echoing the findings of ERT (see Table B-2).

The magnitude of the main effect in our preferred specification in column 3 has a straightforward interpretation, given the log transformation of the rainfall deficit and the standardization of IBLI coverage at the neighborhood level. A one percentage point increase in the rainfall deficit is associated with a 6.76 percentage point increase in the conflict probability for the average IBLI coverage in the neighborhood.[14] If IBLI coverage increases by one standard deviation, the same rain deficit only leads to a 6.76 - 1.74 = 5.02 percentage point increase. Compared to the baseline likelihood of conflict in a cell (roughly 2.5%), a reduction of 1.74 percentage points is an economically relevant effect. Another way of interpreting the effect is that one standard deviation higher IBLI coverage reduces the rainfall-conflict semi-elasticity of about 26% (14% based on the results in column 4).

TABLE I
Baseline results: ITT effect

	Dependent variable: Conflict$_{i,t}$			
	(1)	(2)	(3)	(4)
NEIGHBORHOOD				
Rain deficit (δ_1)	0.0781**		0.0676**	0.0798***
	(0.0341)		(0.0294)	(0.0263)
IBLI (δ_2)		-0.0190***	-0.0278***	-0.0177***
		(0.0044)	(0.0052)	(0.0043)
Rain deficit × IBLI (δ_3)			-0.0174***	-0.0113**
			(0.0053)	(0.0048)
CELL				
Rain deficit (β_1)	-0.0075		-0.0087	-0.0081
	(0.0059)		(0.0059)	(0.0053)
IBLI (β_2)		-0.0076*	-0.0412***	-0.0193
		(0.0046)	(0.0144)	(0.0141)
Rain deficit × IBLI (β_3)			0.0144***	0.0067
			(0.0049)	(0.0045)
Dep. var. mean	0.0245	0.0245	0.0245	0.0245
Cell-fixed effects	✓	✓	✓	✓
Time-fixed effects	✓	✓	✓	✓
IBLI-areas-year-fixed effects	–	–	–	✓
Obs	93400	93400	93400	93400

Notes: The table reports the results of regressing the probability of conflict at the cell level on the rain deficit (log(rainfall)×-1), Index-Based Livestock Insurance (IBLI) coverage, and the respective interaction at the cell and neighborhood level. The neighborhood variables are based on the 1/distance weighting scheme. Rainfall data comes from NASA's GMP product (Huffman et al., 2017). Data on IBLI coverage was provided by the International Livestock Research Institute (ILRI) and conflict data from ACLED (Raleigh et al., 2020). The different variables are processed at a $0.1^\circ \times 0.1^\circ$ grid-cell level. Conley standard errors are implemented using the acreg package in Stata (Colella et al., 2019), with a distance cutoff of 200km. * $p < 0.1$, ** $p < 0.05$, *** $p < 0.01$

The coefficients of the cell-level covariates, which serve mostly as control variables for us, align with the previous literature. MN find a negative correlation of the rain deficit at a location itself with conflict. Their interpretation is that pastoralists are driven by the search for

[14] This effect is about 1.5 times the size of the average effect for all of Africa that MN find in their study for rainfall changes on neighboring pastoral homelands.

forage and are thus less likely to move to a location that cannot provide it due to less rainfall. In contrast, following the opportunity cost argument, less rain could lead to less income and, therefore, more conflict in the cell itself. Like MN, we find a negative coefficient of rain deficit in the cell itself, but it is small and not statistically significant. IBLI coverage in the cell itself, which buffers against income shocks and raises the opportunity costs of fighting, shows a negative and statistically significant coefficient. Without attaching a causal interpretation to this, it is reassuring for the interpretation of our main results that there are at least no adverse effects of IBLI in the cell itself.

In addition to the ITT effect, we can use an instrumental variable specification to approximate the effect of actual IBLI payouts. This is interesting to validate if the conflict-mitigating effect of IBLI runs through its exogenously determined payouts. Note that there is an important limitation to this analysis. We only have information on the occurrence of payouts in IBLI insurance areas during a period, not the payout amount. We assign a value of one for each cell located in an insurance area that received IBLI payouts and zero otherwise. Hence, this reflects only the extensive margin of insurance payouts and assumes a uniform distribution of payouts within the IBLI area.

In our first stage, we instrument the inverse-distance weighted IBLI payouts in the neighborhood IBLI payout neighborhood$_{i,t}$ (z-standardized to ease interpretation) with the interaction of Rain deficit neighborhood$_{i,t}$ with IBLI cover neighborhood$_{i,t}$.

Column 1 of Table II shows that both IBLI coverage in the neighborhood and the interaction with the rainfall deficit are positively correlated, but we only rely on the interaction as a plausibly exogenous instrument. The relevancy assumption is that the interaction affects payouts, and the exclusion restriction is that it only affects conflict through the payouts. The F-statistics in the first stage is 45.8, well above the common thresholds. This first stage result is again robust to including more conservative IBLI eligible times year fixed effects.

The second stage results in Table II shows a statistically significant conflict-reducing effect of IBLI payouts in the neighborhood on the conflict probability within a cell (see column 2). The result is conditional on controlling for the rain deficit and IBLI coverage as the main effects forming the interacted instrument. It remains qualitatively and quantitatively similar if we allow for insurance-area-period fixed effects in columns 3 and 4. Regarding the magnitude of the effect, a standard deviation increase in IBLI payouts in the neighborhood decreased the cell-level conflict likelihood by about 150% to 200%.

Robustness tests: To verify how sensitive our main results are to varying key assumptions, we run various robustness tests. We account for key aspects highlighted by MN and ERT in their studies on the direct effect of droughts on farmer-herder conflict. In summary, we show that our results are robust to varying assumptions on the computation of the neighborhood measures, to defining the ACLED conflict measure and the type of drought proxy differently, and finally to adding more controls.

First, we address the potential worry that the specific way in which we define the neighborhood measures drives our results. We test if the results are sensitive to using different spatial decays or alternative cut-offs for the Conley standard errors. Figure B-2 shows that

TABLE II
2SLS results: Insurance payouts

	2SLS 1st stage	2SLS 2nd stage	2SLS 1st stage	2SLS 2nd stage
	Dependent variable:			
	IBLI payout	$\text{Conflict}_{i,t}$	IBLI payout	$\text{Conflict}_{i,t}$
	(1)	(2)	(3)	(4)
NEIGHBORHOOD				
Rain deficit (δ_1)	0.0974	0.0726**	0.2713	0.0901***
	(0.2551)	(0.0304)	(0.1958)	(0.0269)
IBLI (δ_2)	0.9893***	0.0166	0.9758***	0.0175
	(0.0748)	(0.0116)	(0.0710)	(0.0139)
Rain deficit × IBLI (δ_3)	0.3800***		0.3066***	
	(0.0559)		(0.0518)	
IBLI payouts (δ_4)		-0.0405***		-0.0345**
		(0.0134)		(0.0158)
Dep. var. mean	0	0.0245	0	0.0245
F-stat 1st stage	45.776		34.682	
Cell controls	✓	✓	✓	✓
Cell-fixed effects	✓	✓	✓	✓
Time-fixed effects	✓	✓	✓	✓
IBLI-areas-year-fixed effects	–	–	✓	✓
Obs	93400	93400	93400	93400

Notes: The table reports the 1st stage results (columns 1 and 3) of regressing the neighborhood weighted IBLI payout indicator (z standardized, with mean zero and standard deviation of 1) on the cell level log of rainfall deficit (log(rainfall)×-1), the IBLI cover indicator, the interaction of the two, as well as the neighborhood level log of rainfall deficit, the neighborhood level IBLI coverage (standardized), and the interaction of the two. The neighborhood variables are based on the 1/distance weighting. Columns 2 and 4 report the second stage results with the probability of conflict ($\text{Conflict}_{i,t}$) as the dependent variable, and where the interaction of the neighborhood level log of rainfall deficit and the neighborhood IBLI coverage is the excluded instrument. Cell level controls are reported in Table B-4. Rainfall data comes from NASA's GMP product (Huffman et al., 2017). The Index-Based Livestock Insurance (IBLI) coverage is given by the International Livestock Research Institute (ILRI) and conflict data from ACLED (Raleigh et al., 2020). Cell-level variables are omitted from the table. The different variables are processed at a $0.1^\circ \times 0.1^\circ$ grid-cell level. Conley standard errors are implemented using the acreg package in Stata (Colella et al., 2019), with a distance cutoff of 200km. * $p < 0.1$, ** $p < 0.05$, *** $p < 0.01$

our results hold for a wide range of weight functions ranging from small decays to steep ones ($distance^{-0,5}$ to $distance^{-1.5}$). Moreover, we plot the resulting t-stats from varying the Conley standard errors with cut-offs between 25 and 400km in Figure B-3. We observe that the interaction effect always keeps a t-stat above two and remains stable when increasing the cutoff from 200km to up to 400km.

Second, we test if our choice of dependent and independent variables drives our results. Figure B-4 shows that we obtain similar results for various subcategories of events or actors included in ACLED, grouping event types following ERT, as well as taking the log of ERT classified events. However, precision is somewhat reduced in part of the specifications due to discarding some conflict observations. Table B-3 shows that our results are qualitatively similar if we use the Aridity Index or Dry Matter Productivity as drought measures.

Third, we show that our interaction coefficient of interest is not driven by some correlation

with cell characteristics and the neighborhood measure. In Table B-5, we add interaction between the neighborhood rainfall deficit and several correlates of IBLI coverage (identified in Figure B-1) such as the log of population, the share of range- and farmland, indicators for different climate and biome zones, poor soil quality, water scarcity, border proximity, and national parks. Our coefficient of interest remains stable throughout all of the specifications. Finally, we replicate the exercise at the neighborhood level, weighing all those covariates with the identical distance decay as IBLI coverage and the rainfall deficit. Again, our results remain stable (see Table B-6). Using a single dimension for poor soil quality also does not alter our results (see Table B-7 and Table B-8).

4.2. Channel: Reduced migratory pressure

Based on the results in Jensen et al. (2017), IBLI has the potential to mitigate drought-induced conflict in at least three ways. First, IBLI helps to smooth and increase pastoralists' incomes, thus increasing the opportunity costs of fighting. Second, IBLI is linked to smaller herd sizes and higher investments in the health of the remaining cattle during droughts. This means that when a drought shock hits, there are fewer cattle to feed, and they are, on average, better equipped to survive the shock. Third, IBLI payouts can enable farmers to buy forage from markets, conditional on market access and overall supply. All factors reduce the migratory pressure, i.e., for a given drought shock, pastoralists migrate not as far away from their traditional routes, reducing the likelihood of conflict.

Our data allows us to directly test the third mechanism by building on the spread-of-violence specification employed by ERT for Africa. We follow ERT and match the actors identified in the geolocalized ACLED conflict events to their ethnic homelands (based on Murdock, 1967), with details provided in Table A-3. The small map in Figure III, panel A depicts the homelands in Kenya together with the conflict event locations for all matched conflict events. We calculate the geographic distance between the event location and the respective homeland centroid for each ethnic group that was involved. Absent time-varying representative data on the actual migration routes of pastoralists, we use the logarithm of this distance as our proxy for migration distance. Finally, we compute the log of the average rain deficit in a period for each homeland, and the area share of a homeland covered by IBLI.

The main map in panel A of Figure III illustrates this approach using the Turkana homeland in the northwest of Kenya. We plot all conflict locations involving the Turkana group within our sample, with different colors indicating the respective severity of the rainfall shortage in the Turkana homeland at the time of the event. Pluses and dots indicate if there was IBLI coverage or not. The example illustrates that the frequency of conflict locations involving the Turkana, on average, decreases in distance to the homeland. If there are more severe droughts (orange and red icons), conflict events occur further away from the homeland. However, for droughts of similar intensity, the distance between the conflict event and the homeland is shorter if there was IBLI coverage (comparing dot- and plus-icons of the same color). Hence, the example aligns with the hypothesis that IBLI mitigates conflict by reducing the migratory pressure on pastoralists.

To systematically test for this mechanism, we estimate the following specification:

$$\begin{aligned}\text{Ln Distance}_{k,i,e,t}^{Homeland} = \delta_1 \text{Rain deficit}_{e,t}^{Homeland} + \delta_2 \text{IBLI}_{e,t}^{Homeland} \\ + \delta_3(\text{Rain deficit}_{e,t}^{Homeland} \times \text{IBLI}_{e,t}^{Homeland}) + \eta_e + \gamma_t + \epsilon_{k,i,e,t}\end{aligned} \tag{3}$$

where $\text{Ln Distance}_{k,i,e,t}^{Homeland}$ is the log of geographic distance between the geolocation of a conflict event k, involving actor i matched to ethnic homeland e that occurs in period t. $\text{Rain deficit}_{e,t}^{Homeland}$ is log averaged rainfall in a homeland during period t, which we multiply by minus one (resulting in the log average rainfall deficit) assigned to all actors i that are matched to homeland e. $\text{IBLI}_{e,t}^{Homeland}$ is the share of the homeland e that IBLI covers during period t for actors i matched to homeland e (again z-standardized with mean zero and variance of one).

η_e are homeland fixed effects that capture time-invariant features of ethnic homelands like their size, border location, or geographic features, which could bias our results if they correlate with the likelihood of receiving IBLI and experiencing droughts. γ_t are time fixed effects that capture period-specific shocks and standard errors $\epsilon_{k,i,e,t}$ are clustered at the homeland level, the level of treatment (Abadie et al., 2023). Our main interest is in δ_1, capturing the effect of the exogenous homeland rainfall shortage, and δ_3, capturing again the extent to which IBLI can mitigate this effect.

Panel B of Figure III plots our coefficients of interest together with a 95% confidence intervals. The black dots show that with our baseline specification, there is a significant negative effect of the homeland rainfall deficit on distance. For average homeland IBLI coverage, this can be translated into a rain deficit-distance elasticity of about 0.39. Increasing IBLI coverage by one standard deviation significantly reduces the elasticity by more than half to 0.17.

We find close to identical effect when replacing the homeland fixed effect with more restrictive actor-type-times-homeland fixed effects. These fixed effects absorb time-invariant differences between different actor-types (unorganized groups, militias or organized groups) linked to a homeland. Homelands differ in the composition of actor-types which could bias our baseline results if it correlates with the reaction to drought and IBLI coverage. Moreover, we can replicate the results when restricting the sample to only actors associated with homelands of pastoralist groups (depicted as blue dots and triangles).[15]

Taken together, this is strong evidence that reducing the migratory pressure on pastoralists is a main mechanism for how index-based insurance like IBLI, with its immediate shock absorbance via preemptive payouts, can reduce conflict.

[15] List A-1 documents which groups are classified as pastoral groups. Our classification roughly corresponds to a transhumant pastoral value of above 0.5 as in MN, or the nomad/pastoral dummy in ERT. Reassuringly the homeland of groups not classified as pastoralists in this way do not receive IBLI coverage.

FIGURE III
Droughts, IBLI, and conflict distance to ethnic homelands in Kenya

(A) Turkana illustration

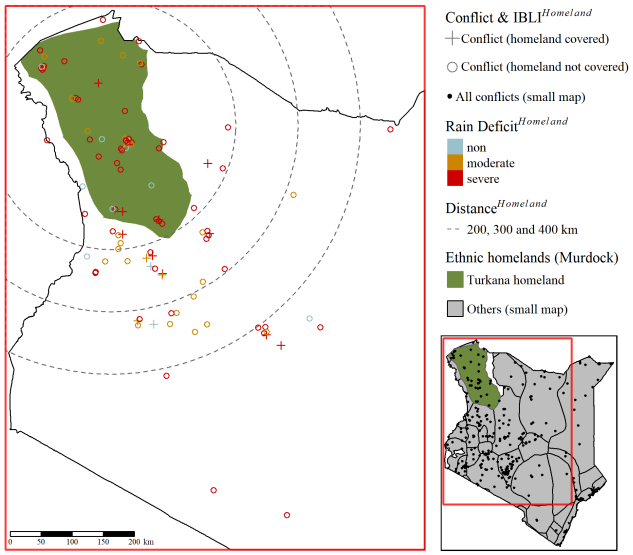

(B) Regression results

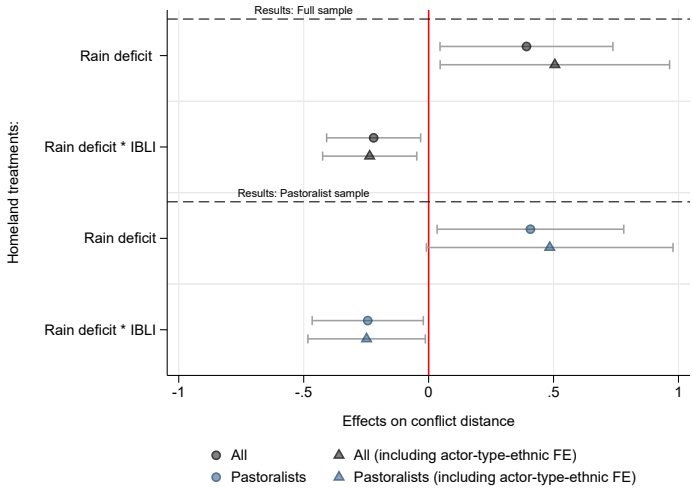

Notes: Panel A of figure plots the conflict locations (ACLED Raleigh et al., 2020) involving Turkana pastoralists over our sample. Different colors indicate the severity of the rainfall deficit (log(rainfall)×-1) in the Turkana homeland (highlighted in green). Blue icons refer to years during abundant rainfall in the Turkana homeland, orange icons refer to locations during moderate droughts in the Turkana homelands, and red icons indicate conflict locations involving Turkana during severe droughts in their homeland. Moreover, the icon type (+ and ○) indicates if the Turkana homeland was covered by IBLI at the time of the conflict event. The Turkana homeland has been covered by IBLI from 2015 onward (homeland area covered at 98% by IBLI since 2015. See panel B of Figure I). The rings show the 200, 300, and 400km distance from the Turkana homeland centroid. The small map in panel A depicts the different Murdock homelands within Kenya (Murdock, 1967) digitized by Nunn (2008). All conflict locations involve actors we could match to members of the ethnic groups traditionally inhabiting the Murdock homelands. Rainfall data comes from NASA's GMP product (Huffman et al., 2017). The Index-Based Livestock Insurance (IBLI) coverage is given by the International Livestock Research Institute (ILRI). Panel B plots the point estimates from our conflict-location homeland-level regressions δ_1 and δ_3 from equation 3. The upper part shows the point estimates and 95% confidence intervals based on our full sample. The lower part shows the results using pastoralist groups only. In both parts of the plot, symbols show the results of the same regression using different fixed effects. ○ represent point estimates including ethnic FE and △ point estimates including an actor-type-ethnic FE. 95% confidence intervals are obtained from standard errors clustered at the homeland (treatment) level. See Table A-3 for details on Actor-Type-Ethnic association and List A-1 for the pastoral classification of ethnic groups.

5. Conclusion

This study, to the best of our knowledge, provides the first causal evidence that index-based livestock insurance (IBLI) can significantly mitigate drought-induced conflict. We find that higher insurance coverage reduces the drought-conflict elasticity between 14% and 26%. Those results are robust to varying all key parameters and using alternative variables and measures. This demonstrates the importance of market-based mechanisms, such as IBLI, in complementing institutional reforms to mitigate the negative effects that climate change is predicted to have on developing countries.

Our analysis also sheds light on the key mechanisms through which IBLI mitigates conflict. IBLI can smooth incomes and increase them by setting incentives to invest in livestock health services and enhanced milk productivity, thus raising the opportunity costs of fighting. The higher productivity per cow also leads to a quantity-quality trade-off and smaller herd sizes in equilibrium, mitigating the rapacity effect. Furthermore, we provide evidence that reduced migratory pressure plays a crucial role. In line with Eberle et al. (2020), we match conflict actors to ethnic homelands (Murdock, 1967) and show that IBLI reduces the distance between a group's homeland centroid and conflict events involving that group. This reduction is more pronounced when focusing on events outside the group's homeland, where most conflicts with farmers occur.

Our findings contribute to the broader literature on conflict-mitigating interventions and the role of technology in development. They highlight the importance of innovative solutions, like remote-sensing-based insurance, in addressing the challenges posed by climate change in conflict-prone settings. By demonstrating the potential of IBLI to reduce conflict and promote economic development, our study provides a strong case for well-designed subsidies and other measures to foster insurance adoption in fragile regions, given the additional positive external effects of IBLI on reducing conflict.

The implications of our analysis extend beyond Kenya to other regions experiencing similar challenges. As climate change continues to threaten fragile ecosystems and livelihoods, it is crucial for governments, international organizations, and the private sector to explore and implement innovative solutions like IBLI. These efforts can help reduce the likelihood of conflict, promote economic development, and improve the resilience of communities affected by climate change.

References

Abadie, A., S. Athey, G. W. Imbens, and J. M. Wooldridge (2023). When should you adjust standard errors for clustering? *Quarterly Journal of Economics 138*(1), 1–35.

Abatzoglou, J. T., S. Z. Dobrowski, S. A. Parks, and K. C. Hegewisch (2018). Terraclimate, a high-resolution global dataset of monthly climate and climatic water balance from 1958–2015. *Scientific Data 5*(1), 1–12.

Acampora, M., L. Casaburi, and J. Willis (2022, September). Land rental markets: Experimental evidence from Kenya. Working Paper 30495, National Bureau of Economic Research.

Andres, A. (2013). Tana river disputes in a drying climate. *Inventory of Conflict and Environment 274*.

Bazzi, S. and C. Blattman (2014). Economic shocks and conflict: Evidence from commodity prices. *American Economic Journal: Macroeconomics 6*(4), 1–38.

Benami, E., Z. Jin, M. R. Carter, A. Ghosh, R. J. Hijmans, A. Hobbs, B. Kenduiywo, and D. B. Lobell (2021). Uniting remote sensing, crop modelling and economics for agricultural risk management. *Nature Reviews Earth & Environment 2*(2), 140–159.

Berman, N. and M. Couttenier (2015). External shocks, internal shots: the geography of civil conflicts. *Review of Economics and Statistics 97*(4), 758–776.

Berman, N., M. Couttenier, D. Rohner, and M. Thoenig (2017). This mine is mine! how minerals fuel conflicts in Africa. *American Economic Review 107*(6), 1564–1610.

Berman, N., M. Couttenier, and R. Soubeyran (2021). Fertile ground for conflict. *Journal of the European Economic Association 19*(1), 82–127.

Blattman, C. (2022). *Why we fight: The roots of war and the paths to peace*. Penguin, London.

Blumenstock, J. E. (2016). Fighting poverty with data. *Science 353*(6301), 753–754.

Cao, Y., B. Enke, A. Falk, P. Giuliano, and N. Nunn (2021, September). Herding, warfare, and a culture of honor: Global evidence. Working Paper 29250, National Bureau of Economic Research.

Casaburi, L., M. Kremer, S. Mullainathan, and R. Ramrattan (2019, September). Harnessing ICT to increase agricultural production: Evidence from Kenya. Working paper, Private Enterprise Development in Low-Income Countries.

Casaburi, L., M. Kremer, and R. Ramrattan (2019, October). Crony capitalism, collective action, and ICT: Evidence from Kenyan contract farming. Working paper, Private Enterprise Development in Low-Income Countries.

Casaburi, L. and J. Willis (2018). Time versus state in insurance: Experimental evidence from contract farming in Kenya. *American Economic Review 108*(12), 3778–3813.

Chantarat, S., A. G. Mude, C. B. Barrett, and M. R. Carter (2013). Designing index-based livestock insurance for managing asset risk in northern Kenya. *Journal of Risk and Insurance 80*(1), 205–237.

Chelanga, P., D. Khalai, F. Fava, and A. Mude. Determining insurable units for index-based livestock insurance in northern Kenya and southern Ethiopia. ILRI Research Brief 83, ILRI, Nairobi, Kenya.

Colella, F., R. Lalive, S. O. Sakalli, and M. Thoenig (2019, August). Inference with arbitrary clustering. Discussion Paper 12584, IZA Institute of Labor Economics.

Couttenier, M. and R. Soubeyran (2014). Drought and civil war in sub-Saharan Africa. *Economic Journal 124*(575), 201–244.

Dube, O. and J. F. Vargas (2013). Commodity price shocks and civil conflict: Evidence from Colombia. *Review of Economic Studies 80*(4), 1384–1421.

Eberle, U. J., D. Rohner, and M. Thoenig (2020, December). Heat and hate: Climate security and farmer-herder conflicts in Africa. Discussion Paper 15542, Centre for Economic Policy Research.

Fabregas, R., M. Kremer, and F. Schilbach (2019). Realizing the potential of digital development: The case of agricultural advice. *Science 366*(6471), p. eaay3038.

FAO (2018). *Pastoralism in Africa's drylands: reducing risks, addressing vulnerability and enhancing resilience.* Food and Agriculture Organization of the United Nations (FAO), Rome, Italy.

Fava, F. and A. Vrieling (2021). Earth observation for drought risk financing in pastoral systems of sub-Saharan Africa. *Current opinion in environmental sustainability 48*, 44–52.

Fava, F. P., D. Nathaniel, J. Sina, G. Andrew, and B. Maher (2021). *Building financial resilience in pastoral communities in Africa: Lessons learned from implementing the Kenya Livestock Insurance Program (KLIP)*. World Bank, Washington, D.C.

Flintan, F. E., R. Behnke, and C. Neely (2013). Natural resource management in the drylands in the horn of Africa: Brief prepared by a technical consortium hosted by CGIAR in partnership with the FAO investment centre. *Technical Consortium Brief*.

Gehring, K., S. Langlotz, and K. Stefan (2023). Stimulant or depressant? Resource-related income shocks and conflict. *Review of Economics and Statistics*, Forthcoming.

H.-O. Pörtner, D.C. Roberts, M. T. E. P. K. M. A. A. M. C. S. L. S. L. V. M. A. O. B. R. e. (2022). *IPCC, 2022: Climate Change 2022: Impacts, Adaptation, and Vulnerability. Contribution of Working Group II to the Sixth Assessment Report of the Intergovernmental Panel on Climate Change*. Cambridge, UK and New York, USA: Cambridge University Press.

Hodler, R., P. Schaudt, and A. Vesperoni (2023, January). Mining for peace. Discussion Paper 17807, Centre for Economic Policy Research.

Huffman, G., E. Stocker, D. Bolvin, E. Nelkin, and J. Tan (2017). Gpm imerg final precipitation l3 1 month 0.1 degree x 0.1 degree v06. *Greenbelt, MD, Goddard Earth Sciences Data and Information Services Center (GES DISC)*. Available at: 10.5067/GPM/IMERG/3B-MONTH/06 Accessed: (11/13/2022).

Jensen, N. D., C. B. Barrett, and A. G. Mude (2017). Cash transfers and index insurance: A comparative impact analysis from northern Kenya. *Journal of Development Economics 129*, 14–28.

Koubi, V. (2019). Climate change and conflict. *Annual Review of Political Science 22*, 343–360.

McGuirk, E. and M. Burke (2020). The economic origins of conflict in Africa. *Journal of Political Economy 128*(10), 3940–3997.

McGuirk, E. F. and N. Nunn (2022). Development missmatch: Land use conversions in pastoral Africa. Mimeo, Tufts University.

McGuirk, E. F. and N. Nunn (2023). Transhumant pastoralism, climate change, and conflict in Africa. *Review of Economic Studies*, Forthcoming.

Michalopoulos, S. and E. Papaioannou (2016). The long-run effects of the scramble for Africa. *American Economic Review 106*(7), 1802–1848.

Miguel, E., S. Satyanath, and E. Sergenti (2004). Economic shocks and civil conflict: An instrumental variables approach. *Journal of Political Economy 112*(4), 725–753.

Morelli, M. and D. Rohner (2015). Resource concentration and civil wars. *Journal of Development Economics 117*, 32–47.

Moscona, J., N. Nunn, and J. A. Robinson (2020). Segmentary lineage organization and conflict in Sub-Saharan Africa. *Econometrica 88*(5), 1999–2036.

Murdock, G. P. (1967). Ethnographic atlas: A summary. *Ethnology 6*(2), 109–236.

Nunn, N. (2008). The long-term effects of Africa's slave trades. *Quarterly Journal of Economics 123*(1), 139–176.

Raleigh, C., A. Linke, and C. Dowd (2020). Armed Conflict Location and Event Dataset (ACLED). *Codebook Version 2*.

Rohner, D. (2022). Mediation, military and money: The promises and pitfalls of outside interventions to end armed conflicts. *Journal of Economic Literature*.

Sundberg, R. and E. Melander (2013). Introducing the UCDP Georeferenced Event Dataset.

Journal of Peace Research 50(4), 523–532.

Vrieling, A., M. Meroni, A. Shee, A. G. Mude, J. Woodard, C. K. de Bie, and F. Rembold (2014). Historical extension of operational NDVI products for livestock insurance in Kenya. *International Journal of Applied Earth Observation and Geoinformation 28*, 238–251.

Online appendix – Insuring Peace: Index-based livestock insurance, droughts, and conflict

Appendices

A. Data Appendix

Measures of conflict

- Conflict$_{i,t}$: Indicator variable that is one if at least one conflict event is recorded in a cell in a given year.
- *I(battle)*: Indicator that is one if at least one battle event occurs in a given year and cell.
- *I(riot)*: Indicator that is one if at least one riot event occurs in a given year and cell.
- *I(civilians)*: Indicator that is one if at least one violence against civilians occurs in a given year and cell.
- *I(gov)*: Indicator that is one if at least one conflict involving the State occurs in a given year and cell.
- *I(pastoral)*: Indicator that is one if at least one event involving a pastoral group is involved in a given year and cell.
- *I(ERT)*: Indicator that is one if at least one event involving a pastoral group is involved in a given year and cell, following the method of Eberle et al. (2020).

Source: ACLED (Raleigh et al., 2020)

IBLI

- *IBLI coverage*: Indicator variable that is one if the centroid of a cell is located within an insurance district that offers the Index-Based Livestock Insurance (IBLI) in a given year.
- *IBLI eligible*: Indicator variable that is one if the centroid of a cell is located within an insurance district that is eligible to the Index-Based Livestock Insurance (IBLI) in a given year.
- *IBLI payouts:* Indicator variable that is one if the centroid of a cell is located within an insurance district that received payouts from the Index-Based Livestock Insurance (IBLI) in a given year.
- *IBLI cover (ever):* Indicator variable that is one if the centroid of a cell is located within an insurance district that is (or will be) covered by the Index-Based Livestock Insurance (IBLI) over our sample period.

Source: The International Livestock Research Institute (ILRI)

Pastoral area: Indicator variable that is one if the centroid of a cell is located within a county with a subnational pastoral population defined as a member county of the Pastoralist Parliamentary Group (PPG).

Pastoralist: Indicator variable that is one if an ethnic group follows the nomad classification in (Eberle et al., 2020), roughly a transhumant pastoralists value of 0.5 and higher in McGuirk and Nunn (2023).

Rain: Continuous variable indicating the mean precipitation in millimeters per year for a given cell. *Source:* NASA's GMP product (Huffman et al., 2017).

Rain deficit: Continuous variable constructed by taking minus the logarithm of annual mean precipitation (*Rain*) for a given cell. *Source:* NASA's GMP product (Huffman et al., 2017)

Dry Matter Productivity (DMP): Continuous variable indicating the overall growth rate or dry biomass increase of the vegetation (kg/ha/year) for a given cell. *Source:* Copernicus Global Land Service (2019)

Aridity index (AI): Continuous variable reconstructed following the definition by the World Atlas Desertification (WAD). The Aridity Index (AI) is a simple but convenient numerical indicator of aridity based on long-term climatic water deficits and is calculated as the ratio of precipitation (P) over Potential Evapotranspiration (PET). The index is computed using monthly data provided by the TerraClimate dataset and aggregated at cell year level. *Source:* World Atlas Desertification (Cherlet, 2018), TerraClimate (Abatzoglou et al., 2018)

Rangeland/Farmland/Fringe: Categorical variable indicating the land use type for a given cell based on remotely sensed official land use classifications from 1972-1980. *Source:* Land use map of Kenya. Government of Kenya 1983.

Climate zones: Categorical variable indicating the Köppen-Geiger climate class associated to each cell. *Source:* Present and future Köppen-Geiger climate classification maps at 1-km resolution. (Beck et al., 2018)

Biomes: Categorical variable indicating the terrestrial ecoregions associated to each cell. *Source:* Terrestrial ecoregions of the world: a new map of life on Earth (Olson et al., 2001)

Protected area: Indicator variable that is one if most of the grid area is covered by a protected area for a given year. *Source:* UNEP-WCMC (2022)

River

- *primary river*: Indicator variable that is one if a cell includes a primary (perennial) river.
- *secondary river*: Indicator variable that is one if a cell includes a secondary (non perennial/intermittent/fluctuating) river.

Source: https://geoportal.icpac.net/layers/geonode:ken_water_lines_dcw

National border: Indicator variable that is one the centroid of a cell is located within 50km of the National border of Kenya.

Water body: Indicator variable that is one if a cell include water bodies such as lakes, reservoir, and lagoon. *Source:* https://datacatalog.worldbank.org/search/dataset/0040797

Soil Quality (SQ1 - SQ7): Dummy variable that takes value 1 if the soil is of poor quality. For each soil quality (1 to 7), cells associated with classes 3, 4, or 5 (Severe limitations, Very severe limitations, and Mainly non-soil) are considered as poor soil quality. *Source:* Harmonized World Soil Database (HWSD) (Nachtergaele et al., 2009)

Population: Log of population within a cell based on the GHSL population raster data (2000 estimates). *Source:* https://ghsl.jrc.ec.europa.eu/.

Ethnic (tribal) homelands: Ethnic group associated to a cell according to the Ethnographic Atlas. *Source:* Ethnographic Atlas (Murdock, 1967), shapefile (Nunn, 2008)

FIGURE A-1
Landuse and fringe

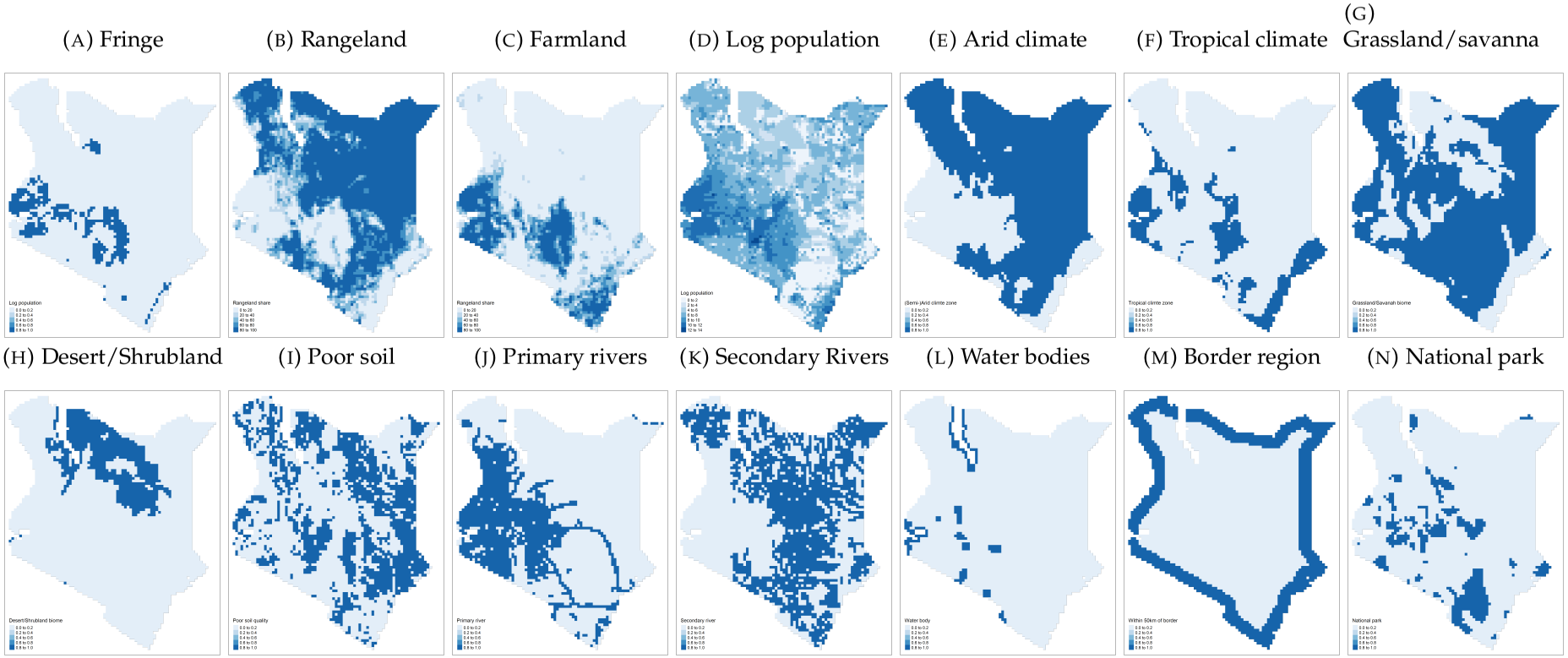

Notes: The fringe indicator (A) are cells considered that are located in both farmland and rangeland area (mixed land use) similar to Eberle et al. (2020) based on Landsat landuse data. The share of rangeland (B) and Farmland (C) are built following the Climate Change Initiative Land Cover (CCI CL) classification (European Space Agency (ESA)). Panel (D) the log of population from the GHSL population raster data (2000 estimates) . Panels (E) to (H) plot our indicator variables for, arid climate zone (E), tropical climate zone (F), grassland or savanna biome (G), desert/shrubland (H) following the Köppen-Geiger climate classification from Beck et al. (2018). Poor soil quality (I) is an indicator variable built using a combination of soil characteristics from the Harmonized World Soil Database (Nachtergaele et al., 2009) where locations associated with class 3, 4, or 5 (severe limitations, very severe limitations, and mainly non-soil) are considered as poor soil quality. Primary (perennial) rivers (J) and secondary (non-perennial/intermittent/fluctuating) rivers (K) are taken from the ICPAC geoportal. Water bodies (L) indicate the presence of lakes, reservoirs, and lagoons from the World Bank database. Border region (M) represents grid-cells located within 50km of the national border of Kenya. National parks (N) are taken from the world database on protected area UNEP-WCMC (2022). All variable are processed at a $0.1° \times 0.1°$ grid-cell level.

TABLE A-1
Summary statistics

Variable	Mean	SD	Min	Max	N
Cell sample					
$\text{Conflict}_{i,t}$	0.02	0.15	0.00	1.00	93,400
I(Gov.)	0.01	0.10	0.00	1.00	93,400
I(NonGov.)	0.02	0.14	0.00	1.00	93,400
I(ERT)	0.02	0.14	0.00	1.00	93,400
Log events (ERT)	0.02	0.16	0.00	4.23	93,400
I(pastoral)	0.00	0.06	0.00	1.00	93,400
I(Battle)	0.01	0.08	0.00	1.00	93,400
I(Riot)	0.01	0.09	0.00	1.00	93,400
I(Civilians)	0.01	0.10	0.00	1.00	93,400
Log rain deficit (cell)	-2.72	0.57	-5.05	-1.10	93,400
Log aridity index deficit (cell)	1.08	0.69	-1.56	3.00	93,400
Log dry matter productivity deficit (cell)	-3.03	0.94	-4.96	0.08	93,000
IBLI coverage (cell)	0.20	0.40	0.00	1.00	93,400
IBLI, eligible (cell)	0.71	0.45	0.00	1.00	93,400
IBLI (coverage ever)	0.60	0.49	0.00	1.00	93,400
Log of population	5.89	3.15	0.00	13.99	93,400
Mixed landuse (farmland and pastoral)	0.10	0.29	0.00	1.00	93,400
Rangeland share (cell)	64.96	37.55	0.00	100.00	93,400
Farmland share (cell)	21.50	32.43	0.00	100.00	93,400
Arid climate	0.70	0.46	0.00	1.00	93,400
Tropical climate	0.17	0.38	0.00	1.00	93,400
Grassland (biome) zone	0.69	0.46	0.00	1.00	93,400
Desert & shrubland (biomes)	0.17	0.37	0.00	1.00	93,400
Poor soil quality	0.41	0.49	0.00	1.00	93,400
Primary river	0.30	0.46	0.00	1.00	93,400
Secondary river	0.49	0.50	0.00	1.00	93,400
Water body	0.04	0.20	0.00	1.00	93,400
National border	0.29	0.46	0.00	1.00	93,400
National park	0.13	0.34	0.00	1.00	93,400
Poor nutrient availability	0.12	0.33	0.00	1.00	93,400
Poor retention capacity	0.03	0.16	0.00	1.00	93,400
Poor rooting condition	0.05	0.23	0.00	1.00	93,400
Poor oxygen availability	0.09	0.29	0.00	1.00	93,400
High excess of salt	0.16	0.36	0.00	1.00	93,400
High toxicity	0.00	0.04	0.00	1.00	93,400
Poor workability condition	0.17	0.38	0.00	1.00	93,400
IBLI coverage (Neighborhood)	-0.00	1.00	-0.75	2.61	93,400
IBLI payouts (Neighborhood)	0.00	1.00	-0.49	4.20	93,400
Log rain deficit (neighborhood)	0.25	0.33	-0.95	1.19	93,400
Log aridity index deficit (neighborhood)	-1.95	0.39	-3.11	-0.75	93,400
Log dry matter productivity deficit (neighborhood)	-6.16	0.36	-6.92	-4.74	93,400
Actor-homeland (Murdock) sample					
Ln distance Actor-location to homeland (conflict)	4.63	0.95	1.55	6.58	1,003
Avg. log rain deficit (homeland)	2.50	0.57	1.43	4.27	1,003
IBLI coverage (homeland)	0.00	1.00	-0.36	3.53	1,003
Pastoral group (homeland)	0.56	0.50	0.00	1.00	1,003

Notes: The table reports the summary statistics of our variables of interests across samples. See Data Appendix A for more details on the variables.

TABLE A-2
Correlation of drought proxies

Panel (A): Cell level cross-correlations			
	Log Rain deficit	Log Aridity index	Log DMP
Log Rain deficit	1		
Log Aridity index	-0.839	1	
Log DMP	-0.811	0.807	1
Panel (B): Neighborhood level cross-correlations			
	Log Rain deficit	Log Aridity index	Log DMP
Log rain deficit	1		
Log Aridity index	-0.906	1	
Log DMP	-0.537	0.567	1

Notes: The table reports the correlations between our different drought proxies. Rain deficit (log(rainfall $\times$ -1)) as been computed using rainfall data from NASA's GMP product (Huffman et al., 2017). The aridity index is the ratio of precipitation over potential evapotranspiration (Abatzoglou et al., 2018). Dry Matter Productivity (DMP) is a phytomass indicator measured by the dry biomass increase of the vegetation (in kg/ha/year, from the Copernicus Global Land Service 2019).

TABLE A-3
ACLED actor, actor type, ethnic group matches

Murdock group	Actor	Actor type
Bararetta	Ajuran Ethnic Militia	Semi-organized
Bararetta	Auliyan Ethnic Militia	Semi-organized
Bararetta	Degodia Ethnic Militia	Semi-organized
Bararetta	Garre Ethnic Militia	Semi-organized
Bararetta	Jibril Clan Militia	Semi-organized
Bararetta	Matan Clan Militia	Semi-organized
Bararetta	Somali Ethnic Militia	Semi-organized
Bararetta	Unidentified Ethnic Militia (Bararetta)	Semi-organized
Bararetta	Unorganized group members (Bararetta)	Unorganized
Bararetta	Wardei Ethnic Militia	Semi-organized
Boni	Abduwak Ethnic Militia	Semi-organized
Boni	Unorganized group members (Boni)	Unorganized
Boran	Borana Ethnic Militia	Semi-organized
Boran	Gabra Ethnic Militia	Semi-organized
Boran	OLF: Oromo Liberation Front	OLF: Oromo Liberation Front
Boran	Orma Ethnic Militia	Semi-organized
Boran	Oromo Ethnic Militia	Semi-organized
Boran	Unorganized group members (Boran)	Unorganized
Dorobo	Kapshoi Clan Militia	Semi-organized
Dorobo	Ndorobo Ethnic Militia	Semi-organized
Dorobo	Ogiek Ethnic Militia	Semi-organized
Dorobo	Unorganized group members (Dorobo)	Unorganized
Gusii	Kisii Communal Militia	Semi-organized
Gusii	Kisii Ethnic Militia	Semi-organized
Gusii	Unorganized group members (Gusii)	Unorganized
Kikuyu	Akorino Sect Militia	Semi-organized
Kikuyu	Kiambu Ethnic Militia	Semi-organized
Kikuyu	Kieleweke	Semi-organized
Kikuyu	Kikuyu Ethnic Militia	Semi-organized
Kikuyu	Mau Mau War Veterans	Semi-organized
Kikuyu	Mungiki Militia	Mungiki Militia
Kikuyu	Unorganized group members (Kikuyu)	Unorganized
Kipsigi	Kipsigi Ethnic Militia	Semi-organized
Kipsigi	Unorganized group members (Kipsigi)	Unorganized
Luo	Luo Ethnic Militia	Semi-organized
Luo	Unorganized group members (Luo)	Unorganized
Masai	Maasai Ethnic Militia	Semi-organized
Masai	Moran Ethnic Militia	Semi-organized
Masai	Siria Clan Militia	Semi-organized
Masai	Unorganized group members (Masai)	Unorganized
Meru	Imenti Ethnic Militia	Semi-organized
Meru	Meru Ethnic Militia	Semi-organized
Meru	Tharaka Ethnic Militia	Semi-organized
Meru	Unorganized group members (Meru)	Unorganized
Nandi	Marakwet Ethnic Militia	Semi-organized
Nandi	Nandi Ethnic Militia	Semi-organized
Nandi	Unorganized group members (Nandi)	Unorganized
Pokomo	Pokomo Ethnic Militia	Semi-organized
Pokomo	Unorganized group members (Pokomo)	Unorganized
Samburu	Isiolo Communal Militia (Samburu)	Semi-organized
Samburu	Pokot Ethnic Militia (Samburu)	Semi-organized
Samburu	Samburu Ethnic Militia	Semi-organized

Continued on next page

Table A-3 – *Continued from previous page*

Murdock group	Actor	Actor type
Samburu	Unorganized group members (Samburu)	Unorganized
Sonjo	Sonjo Ethnic Militia	Semi-organized
Suk	Unorganized group members (Suk)	Unorganized
Topotha	Toposa Ethnic Militia	Semi-organized
Turkana	Turkana Ethnic Militia	Semi-organized
Turkana	Unidentified Ethnic Militia (Turkana)	Semi-organized
Turkana	Unorganized group members (Turkana)	Unorganized
Wanga	Kabasiran Clan Militia	Semi-organized
Wanga	Luhya Ethnic Militia	Semi-organized
Wanga	Unorganized group members (Wanga)	Unorganized

Notes: The table reports the Murdock groups in our sample (Murdock, 1967), the actors reported in ACLED (Raleigh et al., 2020) matched by the association between actor and Murdock groups, and the actor type classification we employ. We classify actors as "unorganized" if they are just members of an ethnic group/tribe but are not organized as a militia. Militias are classified as "semi-organized" because multiple smaller village- or regional militias can be encompassed by the actor name. Actors with an individual name and a formal organization are classified as an individual actor-type (e.g. The Oromo Liberation Front).

LIST A-1
Murdock homelands pastoral/non-pastoral classification

Bajun, Bararetta (P), Boni, Boran (P), Chaga, Didinga (P), Digo, Dorobo (P), Duruma, Gusii, Gyriama, Jie, Kamba, Karamojong (P), Keyu, Kikuyu, Kipsigi, Luo, Masai (P), Meru, Nandi, Pare, Pokomo, Rendile (P), Reshiat (P), Sabei (P), Samburu (P), Sanye (P), Segeju, Shambala, Shashi, Sonjo, Suk (P), Teita, Topotha, Turkana (P), Wanga,

Notes: The list reports our classification of Murdock groups into pastoral and non-pastoral. Groups that are classified as pastoral groups have a (P) next to their name. Our classification corresponds to the nomad classification in (Eberle et al., 2020), roughly a transhumant pastoralists value of 0.5 and higher in McGuirk and Nunn (2023).

B. Additional results

B-1. Additional figures

FIGURE B-1
Balancing results

(A) Ever IBLI eligibility (C)

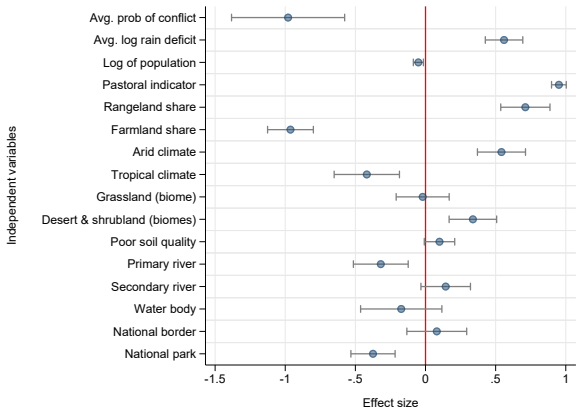

(B) Ever IBLI cover(C)

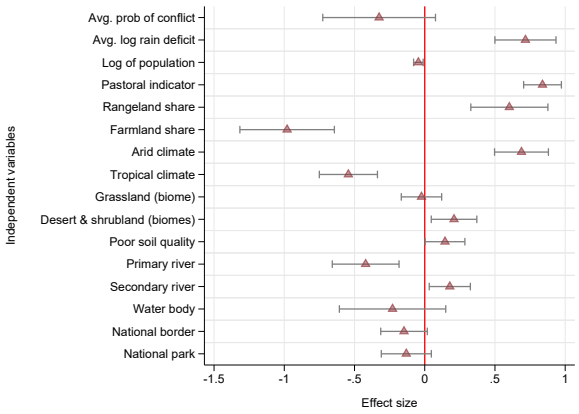

(C) Time to IBLI cover(C)

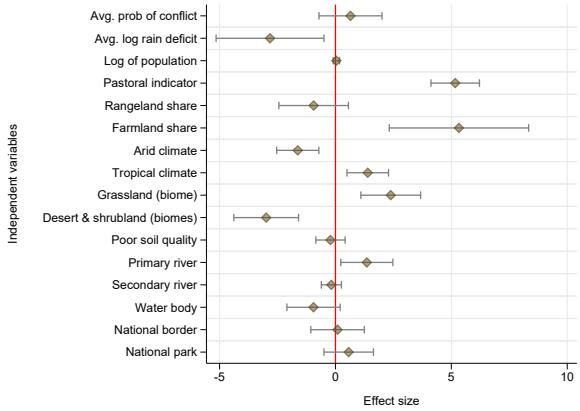

Notes: The figure reports the results from bi-variate balancing tests. We regress the average of a set of variables (depicted on the -axis) between 2001 and 2009 on the probability that a cell is designated to potentially receive IBLI (Panel A). Panel (B) uses a ever-received IBLI coverage indicator, and panel (C) uses a year until coverage received count (from 2010 onward) for the set of cells that are ever covered during our sample period. Index-Based Livestock Insurance (IBLI) coverage is given by the International Livestock Research Institute (ILRI). The average probability of conflict is based on the probability that a conflict event is recorded in a cell during our sample period from ACLED (Raleigh et al., 2020). The log rain deficit is defined as $(\log(\text{rainfall}) \times -1)$ with rainfall data from NASA's GMP product GES DISC (Huffman et al., 2017). The pastoral indicator indicates the presence of pastoralists following the definition of McGuirk and Nunn (2023). Climate zones are defined according to the Köppen-Geiger climate class from Beck et al. (2018). Biomes indicate the terrestrial ecoregions associated to each cell from Olson et al. (2001). Cells with poor soil quality are defined according to the Harmonized World Soil Database (Nachtergaele et al., 2009) (soil characteristics are associated to classes 3, 4 or 5). Primary (perennial) and secondary (non-perennial/intermittent/fluctuating) rivers are from the ICPAC geoportal. Water bodies indicate the presence of lakes, reservoirs, and lagoons based on the World Bank data catalog. National borders are cells with a centroid located within 50km of the border. National Parks are from the world database on protected areas (UNEP-WCMC, 2022). The different variables are processed at a $0.1^\circ \times 0.1^\circ$ grid-cell level. The 95% confidence intervals are based on Conley standard errors, implemented using the acreg package in Stata (Colella et al., 2019), with a distance cutoff of 200km.

FIGURE B-2
Main results: Alternative distance decay neighborhood effects

(A) Rain deficit (Neighborhood) (B) Rain deficit × IBLI (Neighborhood)

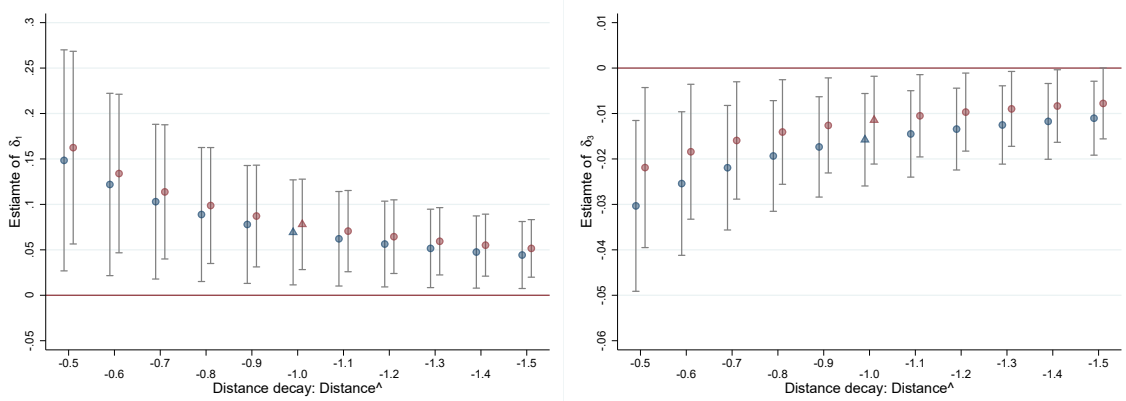

Notes: The figure plots the point estimates and 95% confidence intervals of the log of neighborhood rainfall deficit (log(rainfall) $\times -1$) (panel A), and its interaction with the standardized neighborhood IBLI coverage (panel B) for varying distance decays. The blue circles indicate estimates from replicating column (3) of Table I, and red circles indicate estimates from replicating column 4 of Table I–including klip-area-period fixed effects. Index-Based Livestock Insurance (IBLI) coverage is given by the International Livestock Research Institute (ILRI). Rainfall data comes from NASA's GMP product (Huffman et al., 2017). The different variables are processed at a $0.1^\circ \times 0.1^\circ$ grid-cell level. The confidence intervals in grey are based on Conley standard errors, implemented using the acreg package in Stata (Colella et al., 2019), with a distance cutoff of 200km. $p < 0.1$, $p < 0.05$, $p < 0.01$

FIGURE B-3
Main results: Spatial cutoffs

(A) Cell & year FE (B) Cell & pastoral-area-year FE

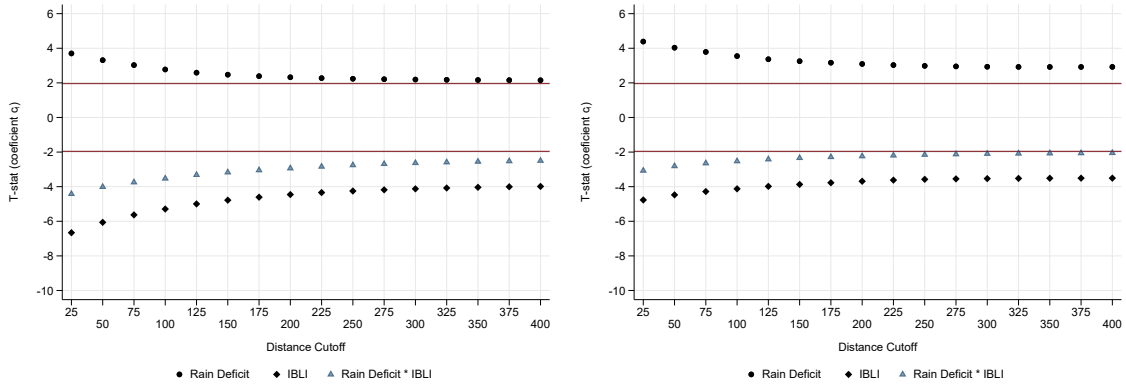

Notes: Panel (A) of the figure plots the t-statistics for our coefficients of interest (δ_1, δ_2, and δ_3) based on our baseline specification (column 3 of Table I for varying distance cutoffs in the spatial clustering. Panel (B) replicates panel (A) but adds IBLI-area-period fixed effects, corresponding to the specification reported in column 4 of Table I. Index-Based Livestock Insurance (IBLI) coverage is given by the International Livestock Research Institute (ILRI). Rainfall data comes from NASA's GMP product (Huffman et al., 2017).

FIGURE B-4
Main results: Alternative conflict measures

(A) Rain deficit (δ_1) (B) Rain deficit $\times$ IBLI (δ_3)

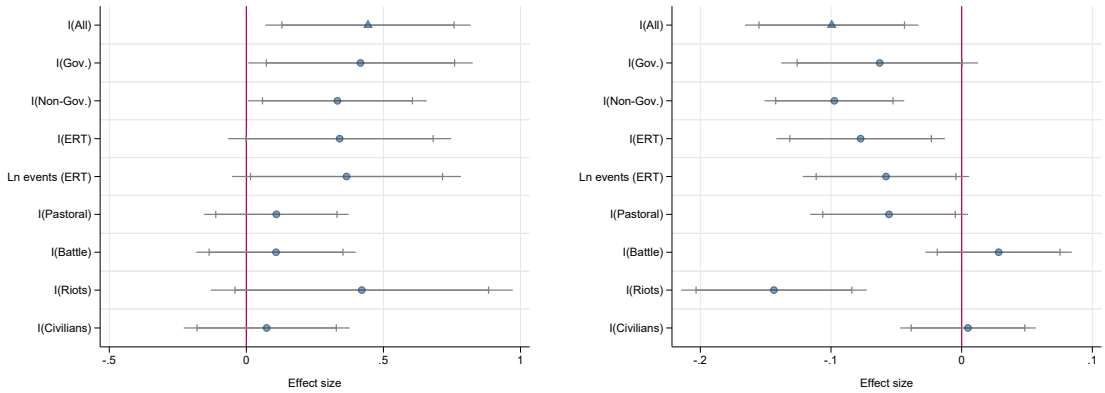

Notes: The figure reports our point estimates of interest (δ_1 and δ_3) and 95% confidence intervals for alternative conflict measures from the ACLED dataset (Raleigh et al., 2020) regressed on the specification in column 3 of Table I. *All* considers all associated actors and types of incidents. *Gov.* are incidents that involve the government (*Non-Gov* when it does not). *ERT* are incidents following the definition of "conflict" by Eberle et al. (2020); an indicator that takes unity when an event is categorized as "Battle", "Violence against civilians", or "Riots". *Riots* are only riots incidents. *Civilians* are incidents involving violent events against civilians. *Pastoral* are incidents that involve an ethnic group defined as pastoralist following the classification by McGuirk and Nunn (2023). Panel (A) reports the obtained δ_1. Panel (B) reports the corresponding δ_3. Index-Based Livestock Insurance (IBLI) coverage is given by the International Livestock Research Institute (ILRI). Rainfall data comes from NASA's GMP product (Huffman et al., 2017). The different variables are processed at a $0.1^\circ \times 0.1^\circ$ grid-cell level. The 95% confidence intervals are based on Conley standard errors, implemented using the acreg package in Stata (Colella et al., 2019), with a distance cutoff of 200km.

B-2. Additional tables

TABLE B-1
IBLI payout in insurance district

	Dependent variable: IBLI payout in insurance area			
	(1)	(2)	(3)	(4)
IBLI	0.4032	1.1732	0.0853	1.4769
	(0.0548)	(0.1085)	(0.0770)	(0.1817)
DROUGHT PROXY				
Rain deficit	0.3147			0.7397
	(0.3116)			(0.3594)
DMP deficit		0.0857		0.0369
		(0.0997)		(0.0807)
AI deficit			-0.3236	-0.1344
			(0.0553)	(0.0664)
DROUGHT PROXY × KLIP AVAILABILITY				
Rain deficit	0.5092			0.3978
	(0.0835)			(0.1127)
DMP deficit		0.2900		0.3029
		(0.0303)		(0.0474)
AI deficit			0.2324	-0.1766
			(0.0464)	(0.0564)
$\text{Conflict}_{i,t+1}$	0.0098	0.0020	0.0086	0.0035
	(0.0339)	(0.0330)	(0.0344)	(0.0306)
$\text{Conflict}_{i,t}$	0.0040	-0.0090	-0.0016	-0.0057
	(0.0297)	(0.0310)	(0.0287)	(0.0286)
$\text{Conflict}_{i,t-1}$	-0.0015	-0.0169	-0.0010	-0.0011
	(0.0348)	(0.0334)	(0.0340)	(0.0334)
Unit-fixed effects	✓	✓	✓	✓
Period-fixed effects	✓	✓	✓	✓
Adj. R2	0.6982	0.7038	0.6913	0.7221
Obs	765	765	765	765

Notes: The table reports the regression results of regressing an indicator for IBLI payouts on different drought proxies; rainfall deficit (log(rainfall) $\times -1$) from NASA's GMP product (Huffman et al., 2017), Dry Matter Productivity deficit (log(DMP) $\times -1$) from the Copernicus Land Service (2019), and the aridity index deficit (ratio of precipitation over potential evapotranspiration, (log(AI) $\times -1$)) from Abatzoglou et al. (2018), as well as their interaction with KLIP availability within insurance districts (or Unit Insurance Area UIA, see Fava et al., 2021) over our periods. Index-Based Livestock Insurance (IBLI) coverage and payouts are given by the International Livestock Research Institute (ILRI) and conflict events from ACLED (Raleigh et al., 2020). The different variables are processed at a $0.1° \times 0.1°$ grid-cell level. Unit-fixed effects are UIA fixed effects. Standard errors are clustered at the IBLI-unit level.

TABLE B-2
Fringe: ITT effect

	Dependent variable: Conflict$_{i,t}$			
	(1)	(2)	(3)	(4)
NEIGHBORHOOD				
Rain deficit (δ_1)	0.0721		0.0643	0.0761
	(0.0309)		(0.0264)	(0.0240)
IBLI (δ_2)		-0.0148	-0.0211	-0.0155
		(0.0043)	(0.0050)	(0.0043)
Rain deficit × IBLI (δ_3)			-0.0121	-0.0085
			(0.0050)	(0.0046)
NEIGHBORHOOD × FRINGE				
Rain deficit (ψ_1)	-0.0330		-0.0228	-0.0321
	(0.0491)		(0.0444)	(0.0379)
IBLI (ψ_2)		0.0201	0.0057	-0.0032
		(0.0064)	(0.0083)	(0.0077)
Rain deficit × IBLI (ψ_3)			-0.0219	-0.0311
			(0.0128)	(0.0119)
Cell-fixed effects	✓	✓	✓	✓
Time-fixed effects	✓	✓	✓	✓
IBLI-areas-year-fixed effect	–	✓	–	✓
Obs	93160	93160	93160	93160

Notes: The table reports the results of regressing our indicator for any conflict event on the log of rainfall deficit (log(rainfall)×-1) at the cell and neighborhood level, the insurance cover indicator at the cell level, the standardized insurance coverage neighborhood measure, and the respective interactions at the cell and neighborhood level. Rainfall data comes from NASA's GMP product (Huffman et al., 2017). The Index-Based Livestock Insurance (IBLI) coverage is given by the International Livestock Research Institute (ILRI) and conflict events from ACLED (Raleigh et al., 2020). In addition, we add interactions of the cell and neighborhood level variables of interest with an indicator variable indicating that a cell is located in the fringe area (defined as mixed land use of farmland and rangeland, similar to Eberle et al. (2020) based on landsat landuse data). The neighborhood variables are based on the 1/distance weighting. The different variables are processed at a $0.1^\circ \times 0.1^\circ$ grid-cell level. Cell-level variables are omitted from the table. Conley standard errors, implemented using the acreg package in Stata (Colella et al., 2019), with a distance cutoff of 200km.

TABLE B-3
ITT effect: Alternative drought proxies

	Dependent variable: Conflict$_{i,t}$			
	(1)	(2)	(3)	(4)
NEIGHBORHOOD				
DMP deficit (δ_1)	0.0218	0.0237		
	(0.0308)	(0.0267)		
DMP deficit × IBLI (δ_3)	-0.0119	-0.0099		
	(0.0042)	(0.0040)		
AI deficit (δ_1)			0.0944	0.1013
			(0.0287)	(0.0260)
AI deficit × IBLI (δ_3)			-0.0124	-0.0075
			(0.0041)	(0.0039)
IBLI (δ_2)	-0.0876	-0.0714	-0.0450	-0.0283
	(0.0262)	(0.0245)	(0.0099)	(0.0086)
Dep. var. mean	0.0245	0.0245	0.0245	0.0245
Cell-fixed effects	✓	✓	✓	✓
Time-fixed effects	✓	–	✓	–
IBLI-areas-year-fixed effects	–	✓	–	✓
Obs	93000	93000	93400	93400

Notes: The table replicates columns 3 and 4 of Table I, switching the rain deficit (log(rainfall)×-1) for alternative drought proxies. In columns 1 and 2, we use a phytomass measure (the Dry Matter Productivity–DMP form the Copernicus Global Land Sevice, 2019). In columns 3 and 4, we leverage the Aridity Index (AI) which is the ratio of precipitation over potential evapotranspiration (with data from Abatzoglou et al. (2018)). As with our rain deficit measure, we log both measures and multiply them by -1 to mimic the scaling of our main specification. The Index-Based Livestock Insurance (IBLI) coverage is given by the International Livestock Research Institute (ILRI) and conflict events from ACLED (Raleigh et al., 2020). The different variables are processed at a $0.1^\circ \times 0.1^\circ$ grid-cell level. Cell level variables are omitted from the output. Conley standard errors are implemented using the acreg package in Stata (Colella et al., 2019), with a distance cutoff of 200km.

TABLE B-4
2SLS results: Cell level controls

	2SLS 1st stage	2SLS 2nd stage	2SLS 1st stage	2SLS 2nd stage
	Dependent variable:			
	IBLI payout	$\text{Conflict}_{i,t}$	IBLI payout	$\text{Conflict}_{i,t}$
	(1)	(2)	(3)	(4)
CELL				
Rain deficit (β_1)	-0.0240	-0.0095	-0.0220	-0.0090
	(0.0579)	(0.0064)	(0.0436)	(0.0057)
IBLI (β_2)	-0.3409	-0.0536	-0.3056	-0.0289
	(0.2226)	(0.0185)	(0.1951)	(0.0173)
Rain deficit × IBLI (β_3)	-0.0315	0.0115	-0.0654	0.0039
	(0.0796)	(0.0052)	(0.0647)	(0.0045)
Dep. var. mean	0	0.0245	0	0.0245
F-stat 1st stage	45.776		34.682	
Cell-fixed effects	✓	✓	✓	✓
Time-fixed effects	✓	✓	✓	✓
IBLI-areas-year-fixed effects	–	–	✓	✓
Obs	93400	93400	93400	93400

Notes: The table reports the cell level controls of Table II. Rainfall data comes from NASA's GMP product (Huffman et al., 2017). The Index-Based Livestock Insurance (IBLI) coverage and payout data are given by the International Livestock Research Institute (ILRI). Conflict events are from ACLED (Raleigh et al., 2020). The different variables are processed at a $0.1° \times 0.1°$ grid-cell level. Cell-level variables are omitted from the table. Conley standard errors are implemented using the acreg package in Stata (Colella et al., 2019), with a distance cutoff of 200km.

TABLE B-5
ITT: Further controls (cell level)

	Dependent variable: Conflict$_{i,t}$									
	(1)	(2)	(3)	(4)	(5)	(6)	(7)	(8)	(9)	(10)
NEIGHBORHOOD										
Rain deficit (δ_1)	0.0718	0.0622	0.0664	0.0544	0.0544	0.0697	0.0665	0.0703	0.0784	0.0686
	(0.0298)	(0.0309)	(0.0292)	(0.0357)	(0.0322)	(0.0297)	(0.0295)	(0.0295)	(0.0296)	(0.0295)
IBLI (δ_2)	-0.0233	-0.0235	-0.0233	-0.0234	-0.0234	-0.0235	-0.0234	-0.0235	-0.0238	-0.0235
	(0.0053)	(0.0053)	(0.0053)	(0.0053)	(0.0053)	(0.0053)	(0.0053)	(0.0053)	(0.0053)	(0.0053)
Rain deficit × IBLI (δ_3)	-0.0157	-0.0158	-0.0162	-0.0160	-0.0166	-0.0153	-0.0155	-0.0152	-0.0173	-0.0153
	(0.0053)	(0.0053)	(0.0054)	(0.0053)	(0.0053)	(0.0052)	(0.0053)	(0.0052)	(0.0053)	(0.0053)
NEIGHBORHOOD RAIN DEFICIT × CELL CHARACTERISTICS										
Ln population	-0.0018									
	(0.0013)									
Share rangeland		0.0001								
		(0.0001)								
Share farmland			-0.0001							
			(0.0001)							
Arid climate zone				0.0104						
				(0.0147)						
Tropical climate zone				-0.0005						
				(0.0147)						
Grassland biome zone					0.0122					
					(0.0104)					
Desert biome zone					0.0219					
					(0.0115)					
Poor soil						-0.0086				
						(0.0088)				
Primary river							-0.0057			
							(0.0073)			
Secondary river							-0.0008			
							(0.0039)			
Water body								0.0236		
								(0.0130)		
Within 50km of border									-0.0150	
									(0.0061)	
National park										0.0045
										(0.0066)
Cell-fixed effects	✓	✓	✓	✓	✓	✓	✓	✓	✓	✓
Time-fixed effects	✓	✓	✓	✓	✓	✓	✓	✓	✓	✓
Obs	93400	93400	93400	93400	93400	93400	93400	93400	93400	93400

Notes: The table reports the results of regressing our indicator for any conflict event (ACLED Raleigh et al., 2020) on the log of rainfall deficit (log(rainfall)×-1) at the cell and neighborhood level, the insurance cover indicator at the cell level, the standardized insurance coverage neighborhood measure, and the respective interactions at the cell and neighborhood level. Rainfall data comes from NASA's GMP product (Huffman et al., 2017). The Index-Based Livestock Insurance (IBLI) coverage is given by the International Livestock Research Institute (ILRI). Throughout columns 1 to 10, we add interactions of the rainfall deficit at the neighborhood level with cell level controls shown as potentially correlated with IBLI coverage (see Figure B-1). Log of population from the GHSL population raster data (2000 estimates). Climate zones follow the Köppen-Geiger climate classification from Beck et al. (2018). Biomes indicate the terrestrial ecoregions from Olson et al. (2001). Poor soil is an indicator variable built using a combination of soil characteristics from the Harmonized World Soil Database (Nachtergaele et al., 2009) where locations associated with class 3, 4, or 5 (severe limitations, very severe limitations, and mainly non-soil) are considered as poor soil quality. Primary rivers (perennial) and secondary (non-perennial/intermittent/fluctuating) rivers are taken from the ICPAC geoportal. Water bodies indicate the presence of lakes, reservoirs, and lagoons from the World Bank database. National parks are taken from the world database on protected area UNEP-WCMC (2022). The neighborhood variables are based on the 1/distance weighting. The different variables are processed at a $0.1^\circ \times 0.1^\circ$ grid-cell level. Cell-level variables are omitted from the table. Conley standard errors are implemented using the acreg package in Stata (Colella et al., 2019), with a distance cutoff of 200km.

TABLE B-6
ITT: Further controls (Neighborhood level)

	Dependent variable: Conflict$_{i,t}$									
	(1)	(2)	(3)	(4)	(5)	(6)	(7)	(8)	(9)	(10)
NEIGHBORHOOD										
Rain deficit (δ_1)	0.0715	0.0634	0.0714	0.0634	0.0682	0.0700	0.0758	0.0841	0.0760	0.0746
	(0.0305)	(0.0295)	(0.0302)	(0.0298)	(0.0294)	(0.0298)	(0.0305)	(0.0295)	(0.0298)	(0.0302)
IBLI (δ_2)	-0.0236	-0.0236	-0.0236	-0.0237	-0.0237	-0.0235	-0.0239	-0.0236	-0.0239	-0.0238
	(0.0053)	(0.0053)	(0.0053)	(0.0053)	(0.0053)	(0.0053)	(0.0053)	(0.0052)	(0.0053)	(0.0053)
Rain deficit × IBLI (δ_3)	-0.0154	-0.0176	-0.0152	-0.0178	-0.0187	-0.0152	-0.0174	-0.0153	-0.0171	-0.0154
	(0.0052)	(0.0058)	(0.0053)	(0.0057)	(0.0058)	(0.0053)	(0.0056)	(0.0052)	(0.0054)	(0.0052)
NEIGHBORHOOD RAIN DEFICIT × NEIGHBORHOOD CHARACTERISTICS										
Ln population	0.0012									
	(0.0049)									
Share rangeland		0.0051								
		(0.0038)								
Share farmland			0.0016							
			(0.0039)							
Arid climate zone				0.0067						
				(0.0041)						
Tropical climate zone				0.0026						
				(0.0033)						
Grassland biome zone					0.0048					
					(0.0031)					
Desert biome zone					0.0063					
					(0.0031)					
Poor soil						-0.0009				
						(0.0020)				
Primary river							0.0050			
							(0.0042)			
Secondary river							0.0050			
							(0.0036)			
Water body								0.0062		
								(0.0039)		
Within 50km of border									-0.0054	
									(0.0031)	
National park										0.0050
										(0.0032)
Cell-fixed effects	✓	✓	✓	✓	✓	✓	✓	✓	✓	✓
Time-fixed effects	✓	✓	✓	✓	✓	✓	✓	✓	✓	✓
Obs	93400	93400	93400	93400	93400	93400	93400	93400	93400	93400

Notes: The table reports the results of regressing our indicator for any conflict event (ACLED Raleigh et al., 2020) on the log of rainfall deficit (log(rainfall)×-1) at the cell and neighborhood level, the insurance cover indicator at the cell level, the standardized insurance coverage neighborhood measure, and the respective interactions at the cell and neighborhood level. Rainfall data comes from NASA's GMP product (Huffman et al., 2017). The Index-Based Livestock Insurance (IBLI) coverage is given by the International Livestock Research Institute (ILRI). Throughout columns 1 to 10, we add interactions of the rainfall deficit at the neighborhood level with neighborhood versions of the cell level controls shown as potentially correlated with IBLI coverage (see Figure B-1). Log of population from the GHSL population raster data (2000 estimates). Climate zones follow the Köppen-Geiger climate classification from Beck et al. (2018). Biomes indicate the terrestrial ecoregions from Olson et al. (2001). Poor soil is an indicator variable built using a combination of soil characteristics from the Harmonized World Soil Database (Nachtergaele et al., 2009) where locations associated with class 3, 4, or 5 (severe limitations, very severe limitations, and mainly non-soil) are considered as poor soil quality. Primary rivers (perennial) and secondary (non-perennial/intermittent/fluctuating) rivers are taken from the ICPAC geoportal. Water bodies indicate the presence of lakes, reservoirs, and lagoons from the World Bank database. National parks are taken from the world database on protected area UNEP-WCMC (2022). The neighborhood variables are based on the 1/distance weighting. The different variables are processed at a $0.1^\circ \times 0.1^\circ$ grid-cell level. Cell-level variables are omitted from the table. Conley standard errors are implemented using the acreg package in Stata (Colella et al., 2019), with a distance cutoff of 200km.

TABLE B-7
ITT: Soil quality controls (cell level)

	Dependent variable: Conflict$_{i,t}$						
	(1)	(2)	(3)	(4)	(5)	(6)	(7)
NEIGHBORHOOD							
Rain deficit (δ_1)	0.0677	0.0685	0.0691	0.0702	0.0680	0.0687	0.0730
	(0.0297)	(0.0296)	(0.0296)	(0.0297)	(0.0297)	(0.0295)	(0.0297)
IBLI (δ_2)	-0.0235	-0.0235	-0.0235	-0.0235	-0.0235	-0.0235	-0.0235
	(0.0053)	(0.0053)	(0.0053)	(0.0053)	(0.0053)	(0.0053)	(0.0053)
Rain deficit × IBLI (δ_3)	-0.0154	-0.0154	-0.0154	-0.0154	-0.0154	-0.0154	-0.0154
	(0.0052)	(0.0052)	(0.0052)	(0.0052)	(0.0052)	(0.0052)	(0.0052)
NEIGHBORHOOD RAIN DEFICIT × POOR SOIL CELL CHARACTERISTICS							
Nutrient availability	0.0042						
	(0.0052)						
Nutrient retention capacity		0.0066					
		(0.0125)					
Rooting condition			-0.0061				
			(0.0081)				
Oxygen availability				-0.0072			
				(0.0066)			
Excess salts					0.0016		
					(0.0039)		
Toxicity						0.0286	
						(0.1033)	
Workability							-0.0127
							(0.0073)
Cell-fixed effects	✓	✓	✓	✓	✓	✓	✓
Time-fixed effects	✓	✓	✓	✓	✓	✓	✓
Obs	93400	93400	93400	93400	93400	93400	93400

Notes: The table reports the results of regressing our indicator for any conflict event (ACLED Raleigh et al., 2020) on the log of rainfall deficit (log(rainfall)×-1) at the cell and neighborhood level, the insurance cover indicator at the cell level, the standardized insurance coverage neighborhood measure, and the respective interactions at the cell and neighborhood level. Rainfall data comes from NASA's GMP product (Huffman et al., 2017). The Index-Based Livestock Insurance (IBLI) coverage is given by the International Livestock Research Institute (ILRI). Throughout columns 1 to 7, we add interactions of the rainfall deficit at the neighborhood level with a poor soil indicator at the cell level based on soil characteristics from the Hamonized World Soil Database (Nachtergaele et al., 2009). For each one of the soil characteristics, a location is considered to be of poor quality when it is associated to class 3, 4 or 5 (severe limitations, very severe limitations, and mainly non-soil). In cases where some locations encompass a soil characteristic defined as both of poor and good quality, we assign to the location the quality that covers most of the area of that location. The neighborhood variables are based on the 1/distance weighting. The different variables are processed at a $0.1^\circ \times 0.1^\circ$ grid-cell level. Cell-level variables are omitted from the table. Conley standard errors are implemented using the acreg package in Stata (Colella et al., 2019), with a distance cutoff of 200km.

TABLE B-8
ITT: Soil quality controls (neighborhood level)

	Dependent variable: Conflict$_{i,t}$						
	(1)	(2)	(3)	(4)	(5)	(6)	(7)
NEIGHBORHOOD							
Rain deficit (δ_1)	0.0657	0.0693	0.0691	0.0692	0.0614	0.0701	0.0675
	(0.0294)	(0.0297)	(0.0295)	(0.0296)	(0.0297)	(0.0289)	(0.0295)
IBLI (δ_2)	-0.0236	-0.0236	-0.0234	-0.0235	-0.0234	-0.0235	-0.0235
	(0.0053)	(0.0053)	(0.0053)	(0.0053)	(0.0053)	(0.0053)	(0.0053)
Rain deficit × IBLI (δ_3)	-0.0158	-0.0155	-0.0155	-0.0153	-0.0166	-0.0154	-0.0160
	(0.0053)	(0.0053)	(0.0053)	(0.0053)	(0.0054)	(0.0052)	(0.0055)
NEIGHBORHOOD RAIN DEFICIT × POOR SOIL NEIGHBORHOOD CHARACTERISTICS							
Nutrient availability	0.0025						
	(0.0024)						
Nutrient retention capacity		0.0012					
		(0.0030)					
Rooting condition			0.0011				
			(0.0030)				
Oxygen availability				-0.0004			
				(0.0025)			
Excess salts					0.0044		
					(0.0030)		
Toxicity						0.0008	
						(0.0047)	
Workability							0.0021
							(0.0038)
Cell-fixed effects	✓	✓	✓	✓	✓	✓	✓
Time-fixed effects	✓	✓	✓	✓	✓	✓	✓
Obs	93400	93400	93400	93400	93400	93400	93400

Notes: The table reports the results of regressing our indicator for any conflict event (ACLED Raleigh et al., 2020) on the log of rainfall deficit (log(rainfall)×-1) at the cell and neighborhood level, the insurance cover indicator at the cell level, the standardized insurance coverage neighborhood measure, and the respective interactions at the cell and neighborhood level. Rainfall data comes from NASA's GMP product (Huffman et al., 2017). The Index-Based Livestock Insurance (IBLI) coverage is given by the International Livestock Research Institute (ILRI). Throughout columns 1 to 7, we add interactions of the rainfall deficit at the neighborhood level with a poor soil indicator at the cell level based on soil characteristics from the Harmonized World Soil Database (Nachtergaele et al., 2009). For each one of the soil characteristics, a location is considered to be of poor quality when it is associated to class 3, 4 or 5 (severe limitations, very severe limitations, and mainly non-soil). In cases where some locations encompass a soil characteristic defined as both of poor and good quality, we assign to the location the quality that covers most of the area of that location. The neighborhood variables are based on the 1/distance weighting. The different variables are processed at a $0.1^\circ \times 0.1^\circ$ grid-cell level. Cell-level variables are omitted from the table. Conley standard errors are implemented using the acreg package in Stata (Colella et al., 2019), with a distance cutoff of 200km.

Additional references

Abatzoglou, J. T., S. Z. Dobrowski, S. A. Parks, and K. C. Hegewisch (2018). Terraclimate, a high-resolution global dataset of monthly climate and climatic water balance from 1958–2015. *Scientific Data 5*(1), 1–12.

Beck, H. E., N. E. Zimmermann, T. R. McVicar, N. Vergopolan, A. Berg, and E. F. Wood (2018). Present and future köppen-geiger climate classification maps at 1-km resolution. *Scientific Data 5*(1), 1–12.

Cherlet, M., H. C. R. J. H. J. S. S. v. M. G. (2018). *World Atlas of Desertification*. Publication Office of the European Union, Luxembourg.

Colella, F., R. Lalive, S. O. Sakalli, and M. Thoenig (2019, August). Inference with arbitrary clustering. Discussion Paper 12584, IZA Institute of Labor Economics.

Eberle, U. J., D. Rohner, and M. Thoenig (2020, December). Heat and hate: Climate security and farmer-herder conflicts in Africa. Discussion Paper 15542, Centre for Economic Policy Research.

Fava, F. P., D. Nathaniel, J. Sina, G. Andrew, and B. Maher (2021). *Building financial resilience in pastoral communities in Africa: Lessons learned from implementing the Kenya Livestock Insurance Program (KLIP)*. World Bank, Washington, D.C.

Huffman, G., E. Stocker, D. Bolvin, E. Nelkin, and J. Tan (2017). Gpm imerg final precipitation l3 1 month 0.1 degree x 0.1 degree v06. *Greenbelt, MD, Goddard Earth Sciences Data and Information Services Center (GES DISC)*. Available at: 10.5067/GPM/IMERG/3B-MONTH/06 Accessed: (11/13/2022).

McGuirk, E. F. and N. Nunn (2023). Transhumant pastoralism, climate change, and conflict in Africa. *Review of Economic Studies*, Forthcoming.

Murdock, G. P. (1967). Ethnographic atlas: A summary. *Ethnology 6*(2), 109–236.

Nachtergaele, F., H. Velthuizen, L. Verelst, and D. Wiberg (2009). Harmonized world soil database (hwsd). *Food and Agriculture Organization of the United Nations, Rome*.

Nunn, N. (2008). The long-term effects of Africa's slave trades. *Quarterly Journal of Economics 123*(1), 139–176.

Olson, D. M., E. Dinerstein, E. D. Wikramanayake, N. D. Burgess, G. V. Powell, E. C. Underwood, J. A. D'amico, I. Itoua, H. E. Strand, J. C. Morrison, et al. (2001). Terrestrial ecoregions of the world: A new map of life on earth: A new global map of terrestrial ecoregions provides an innovative tool for conserving biodiversity. *BioScience 51*(11), 933–938.

Raleigh, C., A. Linke, and C. Dowd (2020). Armed Conflict Location and Event Dataset (ACLED). *Codebook Version 2*.

UNEP-WCMC (2022). Protected area profile for Kenya from the world database on protected areas. Available at: www.protectedplanet.net.